TECHNICAL MEMORANDUM

838

Monitoring and assimilation of early TROPOMI total column carbon monoxide data in the CAMS system

Antje Inness[1], Ilse Aben[2], Anna Agusti-Panareda[1], Tobias Borsdorff[2], Johannes Flemming[1], Jochen Landgraf[2] and Roberto Ribas[1]

Copernicus Department

24 January 2019

[1]ECMWF, Shinfield Park, Reading, RG2 9AX, UK

[2]SRON Netherlands Institute for Space Research, Utrecht, the Netherlands

European Centre for Medium-Range Weather Forecasts
Europäisches Zentrum für mittelfristige Wettervorhersage
Centre européen pour les prévisions météorologiques à moyen

Series: ECMWF Technical Memoranda

A full list of ECMWF Publications can be found on our web site www.ecmwf.int.

Contact: library@ecmwf.int

European Centre for Medium Range Weather Forecasts
Shinfield Park, Reading, Berkshire RG2 9AX, England

Abstract

The Tropospheric Monitoring Instrument (TROPOMI) on the Copernicus Sentinel 5 Precursor (S5P) satellite, launched in October 2017, provides a wealth of atmospheric composition data, including total columns of carbon monoxide (TCCO) at high horizontal resolution (7 km x 7 km) retrieved from the shortwave-infrared (SWIR) part of the solar spectrum. TROPOMI offline TCCO data (V1.0.2) have been included in the data assimilation system of the Copernicus Atmospheric Monitoring Service (CAMS) to assess the quality of the data and to carry out first assimilation tests with the data for the period 28 January to 3 May 2018. Even though S5P was still in its commissioning phase until 24 April 2018 the TROPOMI TCCO data were of good enough quality for these tests.

The TROPOMI data successfully capture the global TCCO distribution as given by the CAMS analysis that routinely assimilates thermal infrared (TIR) TCCO retrievals from the Measurement of Pollution in the Troposphere (MOPITT) instrument and the Atmospheric Sounding Interferometer (IASI). However, there are some biases between the TROPOMI data and the CAMS CO analysis, particularly in the northern hemisphere (NH) at low solar elevations north on 40ºN where TROPOMI has higher TCCO values than CAMS. Relative to CAMS and averaged over the period from 28 January to 3 May 2018, the TROPOMI data have a bias of $0.17 \pm 0.27\ 10^{18}$ molec cm^{-2} in the NH, $-0.07 \pm 0.19\ 10^{18}$ molec cm^{-2} in the Tropics and $0.009 \pm 0.12\ 10^{18}$ molec cm^{-2} in the southern hemisphere (SH).

When TROPOMI data are assimilated in the CAMS system they lead to increased CO values in the Extratropics and lower values in the Tropics, with TCCO changes of up to 30% at high northern latitudes. Even though the TROPOMI data are total columns their assimilation has a large impact on the vertical structure of the CAMS CO analysis, because of different sensitivities of the TROPOMI SWIR and MOPITT and IASI TIR retrievals to CO in the atmosphere

The assimilation of TROPOMI TCCO improves the fit to European Global Atmosphere Watch surface CO observations over Europe and to In-service Aircraft for a Global Observing System aircraft profiles in several areas. Particularly noteworthy is that the assimilation of TROPOMI TCCO leads to increased CO values in the lower troposphere over Europe, where the long standing low bias of the CAMS system is reduced. The fit to data from the Total Carbon Column Observing Network is degraded in the NH, but improved at Lauder in the SH.

1 Introduction

The Copernicus Atmosphere Monitoring Service (CAMS, atmosphere.copernicus.eu) produces daily global real-time forecasts of atmospheric composition up to five days ahead. To improve the quality of the CAMS forecasts the initial conditions for some of the chemical species, including Ozone (O_3), Carbon Monoxide (CO), Nitrogen Dioxide (NO_2), Sulphur Dioxide (SO_2) and for aerosols are provided by assimilating satellite retrievals of atmospheric composition using ECMWF's 4-dimensional variations (4D-Var) data assimilation system (Benedetti et al., 2009; Inness et al., 2013; Inness et al., 2015).

A wealth of new atmospheric composition data has become available with the launch of the Sentinel 5-Precursor (S5P) satellite in October 2017. S5P carries the TROPOspheric Monitoring Instrument

(TROPOMI) which provides high resolution spectral measurements in the ultraviolet (UV), visible (VIS), near infrared (NIR) and shortwave-infrared (SWIR) part of the spectrum. This wide spectral range allows several atmospheric pollutants species to be retrieved, e.g. O_3, NO_2, SO_2 and Formaldehyde (HCHO) from the UVVIS, and CO and Methane (CH4) from the SWIR part of the spectrum (Veefkind et al, 2012). These species are all included in the CAMS system, making TROPOMI the perfect instrument to provide observations for the CAMS real-time analysis at unprecedented horizontal resolution of about 7 km x 7 km for data retrieved from the SWIR band and 3.5 km x 7 km for data from the UVVIS bands. First offline TROPOMI total column CO (TCCO) data produced with the operational algorithm by SRON, the Netherlands Institute for Space Research, have shown a good agreement with the CAMS real-time CO analysis (Borsdorff et al., 2018) with a mean difference between the data sets of 3.2±5.5 % and a correlation coefficient of 0.97 for a period in November 2017. In this paper, we assess the agreement of the TROPOMI TCCO with the CAMS real-time analysis for a longer period from 28 January 2018 to 3 May 2018 by including the offline TROPOMI TCCO data (v1.0.2) in the CAMS system. We also carry out first assimilation tests with the data. TROPOMI S5P has been operational since 25 April 2018, so the data used in this paper are mostly from the so-called commissioning phase which is primarily dedicated to functional testing, in-flight calibration and testing of the processing chain. Nonetheless, quite some Earthshine observations were made between 28 January and 3 May 2018 which allowed us to perform a first testing of TROPOMI TCCO in the CAMS system.

Carbon monoxide has natural and anthropogenic sources (Seinfeld and Pandis, 2006; Kanakidou and Crutzen, 1999). It is emitted from soils, plants and the ocean, but its main sources are incomplete fossil fuel and biomass burning, which lead to enhanced surface concentrations. Another important source of CO is the oxidation of anthropogenic and biogenic volatile organic compounds (VOCs). In areas with large biogenic emissions (e.g. tropical forests), oxidation of biogenic VOCs contributes strongly to the production of CO (Griffin et al. 2007). Hudman et al. (2008) found that over the Eastern US during summer the biogenic sources of CO were higher than the anthropogenic ones due to decreasing anthropogenic emissions. The highest CO concentrations are found over the industrial regions of Europe, Asia and North America. Surface concentrations are higher during the winter than during the summer months because of the shorter lifetime in the summer due to higher concentrations of the hydroxyl radical (OH) and more intense mixing processes. Tropical biomass burning is most intense during the dry season (December-April in the Northern Hemisphere (NH) tropics, July-October in the Southern Hemisphere (SH) tropics). Africa is usually the largest source of CO biomass burning emissions, but under El Niño conditions Asian emissions (and in particular emissions from maritime Southeast Asia) can reach similar values. CO has a lifetime of several weeks and can serve as a tracer for regional and inter-continental transport of polluted air. The main loss process is the reaction with OH.

Before new data are assimilated in the CAMS real-time analysis the quality of the data relative to the current system has to be established. This is usually done by including the data passively in the data assimilation system, so that statistics of the differences between the observations and collocated model fields can be calculated, without the data influencing the analysis and subsequent forecast. We call this ‘monitoring’ of the observations. The model fields are interpolated in time and space to the location of the observations, and the model equivalents of the observations are calculated, e.g. by applying the averaging kernels of the data to the model fields. Temporal and spatial statistics of the differences

between the model fields and the observations can then be investigated. The differences between the observations and the model fields are called departures. We distinguish between first-guess departures (observations minus model first-guess field) and analysis departures (observations minus analysed field). The first guess field is the model forecast from the previous analysis, i.e. before the fields are changed by the analysis increments.

Monitoring the TROPOMI TCCO data with the CAMS data assimilation system enables us to carry out a continuous quality assessment of the data. It allows us to detect biases between TROPOMI and the CAMS analysis as well as between TROPOMI and the other TCCO retrievals that are routinely assimilated in the CAMS system, i.e. TCCO from the Measurement of Pollution in the Troposphere (MOPITT) instrument onboard the Terra satellite and the Infrared Atmospheric Sounding Interferometer (IASI) onboard the Meteorological Operational Satellites (Metop) -A and -B (referred to as IASI-AB below) and will allow us to monitor instrument and algorithm stability. The advantage of using an assimilation system to monitor satellite data is that it provides continuous global coverage and allows us to build up global and regional statistics quickly. If the monitoring shows the data to be of good quality, i.e. departures are stable, there are no sudden jumps, the biases with respect to the model are not too large, assimilation tests with the data usually follow.

This paper is structured in the following way. Section 2 describes the CAMS model and data assimilation system as well as the offline TROPOMI TCCO data (v1.0.2) and how they are included in the CAMS system. Section 3 shows results of monitoring experiments with the TROPOMI TCCO data, results from first assimilation tests with the data and validation of the resulting analyses with independent observations. Section 4 gives the conclusions.

2 Model and observations

2.1 CAMS model and data assimilation system

The CAMS model and data assimilation system is based on the integrated Forecast System (IFS) of the European Centre for Medium Range Weather Forecasts (ECMWF). The chemical mechanism of the IFS is an extended version of the Carbon Bond Mechanism 5 (CB05, Huijnen et al. 2010) as implemented in the Chemical Transport Model (CTM) Transport Model 5 (TM5) and is documented in Flemming et al. (2015) and Flemming et al. (2017). The spatial resolution of the model is approximately 40 km (T511 linear spectral truncation and 0.35° by 0.35° grid), i.e. coarser than the resolution of the TROPOMI TCCO data. The CAMS system uses MACCity anthropogenic emissions (Granier et al., 2011), biomass burning emissions from the Global Fire Assimilation System (GFAS, Kaiser et al., 2012) and biogenic emissions form the Model of Emissions of Gases and Aerosols from Nature (MEGAN, Guenther et al., 2006).

The IFS uses an incremental 4D-Var data assimilation system going back to Courtier et al. (1994). The data assimilation system for the atmospheric composition fields remains unchanged to the one described in Inness et al. (2015). The atmospheric composition fields are included in the control vector and minimized together with the meteorological control variables. The CAMS real-time analysis uses 12-hour assimilation windows from 03 UTC to 15 UTC and 3 UTC to 15 UTC and two minimisations at spectral truncations T95 (~ 210 km) and T159 (~ 110 km).

MOPITT and IASI TCCO data are routinely assimilated in the CAMS real-time system (see Table 1). The MOPITT data we use are the thermal infrared (TIR) V7 MOPITT retrievals from the 4.7 µm band (Deeter et al., 2017). IASI TCCO is retrieved from the same band (spectral range 2143-2181.25 cm^{-1}) and the data used during the period covered in this paper are produced by LATMOS/ULB with the Fast Optimal Retrievals on Layers for IASI (FORLI) algorithm, documented in George et al. (2009) and Clerbaux et al. (2009) and also used in Inness et al. (2013). The TIR retrievals have the largest sensitivity to CO in the mid troposphere (Deeter et al., 2013; George et al., 2015). In the CAMS system, the IASI and MOPITT TCCO data are thinned to a horizontal resolution of 0.5° x 0.5° by randomly selecting an observation in each grid box.

The observation operator for TCCO in the CAMS system applies the averaging kernels of the observations to the model fields and calculates the model equivalent at the observation locations, giving departures between the observations and the model as:

$$d = y - \widehat{H}(x_m) = x_{ap} + A(x_t - x_{ap}) - \left(x_{ap} + A(H(x_m) - x_{ap})\right) = A(x_t - H(x_m)) \quad (1)$$

where d is the departure, y the observed TCCO retrieval, $\widehat{H}$ the observation operator, x_{ap} the apriori profile used during the retrieval of y, x_t the 'true' state of the atmosphere, x_m the model profile, A the averaging kernel and H an operator to calculate CO integrated layers corresponding to the averaging kernels from the model CO profiles. Using this observation operator, we remove the influence of the a-priori profile (see equation 1) because we use the averaging kernels to sample the model profiles according to the assumptions made in the retrieval. However, x_{ap} is still needed in the observation operator calculations.

A variational bias correction (VarBC) scheme (Dee and Uppala, 2009) where biases are estimated during the analysis by including bias parameters in the control vector is used for the TCCO data. In this scheme, the bias corrections are continuously adjusted to optimize the consistency with all information used in the analysis. VarBC is applied to the IASI-AB TCCO data, with the 1000-300 hPa thickness, the thermal contrast between the surface temperature and the temperature of the lowest model level, and a global constant as predictors. MOPITT TCCO data are used to anchor the bias correction, i.e. are assimilated without correction. Experience has shown that it is important to anchor the bias correction, to avoid drifts in the model fields (Inness et al., 2013).

CAMS real-time data are routinely validated and validation reports are produced every three months (https://atmosphere.copernicus.eu/global-services). These reports show that the seasonality of the CO field is reproduced well by the operational CAMS real-time system, i.e. currently still without the assimilation of TROPOMI data, when compared with independent data. Compared to IAGOS aircraft data the shapes of the CO profiles are well reproduced by CAMS, but values are generally smaller than observed. The largest underestimation is found in the lower troposphere, especially over Europe, North America and East Asia where values during the winter can be underestimated by up to -25% (Frankfurt airport) and -40% (East Asian airports). This is also seen in the reanalyses of atmospheric composition that were produced by CAMS (Flemming et al., 2017; Inness et al.; 2018). During the summer months CO can be overestimated in Asia near the surface. Biases against GAW surface observations also show an underestimation in Europe and Asia (up to -30%) during winter and spring. Compared to NDACC FTIR data that measure the CO column between the surface and 20 km the CAMS real-time system

underestimates the CO column in the Northern hemisphere (NH) with relative mean biases below -10% and overestimates it in the Southern Hemisphere (SH) with mean relative biases up to 10%.

2.2 TROPOMI TCCO data

TROPOMI has a local overpass time of 13:30 UTC, a spatial resolution of 7 km x 7 km (in nadir) for data retrieved from the SWIR band, a swath of 2600 km and provides daily global coverage with 14 orbits per day. For the work in this paper we use offline TROPOMI CO data (V1.0.2) for the period 28 January to 3 May 2018.

The TROPOMI TCCO retrieval is documented in Landgraf et al. (2016). The retrieval works in the 2.3 μm spectral range of the SWIR part of the solar spectrum. While the TIR measurements like MOPITT and IASI are mostly sensitive to CO in the mid troposphere (Deeter et al., 2013), TROPOMI SWIR measurements are sensitive to the integrated amount of CO along the light path, including the contribution of the planetary boundary layer, making them particularly suitable for detecting surface sources of CO.

The TROPOMI CO retrieval deploys the profile scaling approach described in detail by Borsdorff et al. (2014). The forward calculation of the measurement is accounting for light scattering by clouds and aerosols in the atmosphere and thus simultaneously retrieves trace gas columns and effective parameters describing the cloud contamination of the measurements (height scattering layer, scattering optical thickness) as demonstrated by Vidot et al. (2012). The TROPOMI TCCO datasets provide total column averaging kernels for individual measurements that describe the vertical sensitivity of the retrieved CO columns. The CO retrieval under clear-sky atmospheric condition shows a good sensitivity throughout the atmosphere with minor variation due to the observation geometry of the satellite. Retrievals from cloud-contaminated measurements exhibit a reduced vertical sensitivity caused by shielding of the cloud in the observation geometry of the satellite. A preliminary validation of the TROPOMI TCCO dataset shows compliance with the mission requirements on accuracy (< 15%) and precision (<10%) although it is slightly biased high compared to ground-based CO column measurements provided by the TCCON network (Borsdorff et al. (2018b).

In this study, we apply the following two quality checks to the data:

1. Pixels with a height_scattering_layer > 5000m are rejected.
2. Pixels with viewing_zenith_angle> 65º and solar_zenith_angle< 80º are rejected.

Data that pass these checks are flagged as ‘good’ and used for the studies presented here. We use clear and cloudy data. In future retrieval versions, a quality flag (‘qa-flag’) will allow the user to filter out good quality data as well as identify clear and cloudy pixels, but this was not the case yet in V1.0.2.

Because the horizontal resolution of the TROPOMI TCCO data (7 km x 7 km) is higher than the model resolution of T511 (about 40 km x 40 km) the TROPOMI data are not spatially representative for the model grid boxes. To overcome this representativeness error, the data are converted into so called ‘super-observations’ before they are included in the CAMS system. For this super-obbing the data are averaged to the T511 resolution of the model. The averaging is carried out separately for different surface types (e.g. land, ocean, ice etc.) and the errors and averaging kernels of the data are averaged in the same way as the observations. The super-obbing reduces the random errors in the data. An example of TROPOMI CO at full resolution and super-obbed to T511 is shown in Figure 1. The super-obbing

reduces the number of TROPOMI observations by about a factor of 10, from about 3 million observations to about 300,000 per day.

3 Results

Two experiments were run with TROPOMI offline TCCO data (V1.0.2) super-obbed to T511 horizontal resolution for the period 28 January to 3 May 2018 using model cycle 45r1 of the IFS. In the first control experiment (CTRL) the TROPOMI data were included passively in the CAMS system, in the second one (ASSIM) the data were actively assimilated north of 65ºS, at solar elevations greater than 25º in the northern hemisphere and if they passed the quality checks described in Section 2.2. MOPITT and IASI-AB TCCO data were assimilated in both experiments (see Table 1).

3.1 Monitoring of TROPOMI CO data

Figure 2 shows the mean TCCO fields averaged over the period from 28 January to 3 May 2018 from TROPOMI and from the other three TCCO datasets that are routinely assimilated in the CAMS real-time system (i.e. MOPITT and IASI-AB). For TROPOMI 'good' data (see section 2.2) super-obbed to T511 are shown, while for the other 3 instruments 'used' data are shown, i.e. the data that passed all quality and blacklist checks (see Table 1) and were actively assimilated. The figure shows that TROPOMI TCCO values agree well with the other datasets and capture the higher TCCO values in the NH, the lower values in the SH, high TCCO values over the biomass burning areas in the Tropics and the areas of high anthropogenic pollution over India and South East (SE) Asia.

Difference plots of TROPOMI and the other three data sets are shown in Fig. 3 and illustrate that there are noticeable differences between the data sets. Because the near real-time MOPITT data are flagged as 'bad' poleward of 65º, the comparison with TROPOMI is limited to the regions equatorward of 65º. TROPOMI has higher TCCO values than MOPITT at high northern latitudes over land (e.g. Canada, Siberia), over Tropical Africa and parts of SE Asia, and lower values in the SH, over the US, North Africa and Europe. The differences between TROPOMI and IASI are larger, with TROPOMI higher than IASI at high northern latitudes over land and over SE Asia. Elsewhere, TROPOMI is lower than IASI with the largest negative differences in the Tropics and over Antarctica (where the retrieval quality of both data sets is poorer). When looking at these differences it has to be born in mind that TROPOMI has a different sensitivity to CO in the troposphere compared to MOPITT and IASI and that at least some of the differences seen here will stem from that. Also, differences in the a-priori profiles used in the retrievals will play a role (George et al., 2015).

Figure 4 shows maps of the standard deviations of the observations over the period 28 January to 3 May 2018 from the four TCCO datasets. Again, TROPOMI data look reasonable and similar to the other data. High variability is found over the tropical biomass burning areas, India and SE Asia, and over the North Pacific and part of the North Atlantic where CO rich air is transported eastwards from the pollution areas of SE Asia and the Eastern US. MOPITT shows similar patterns to TROPOMI but slightly lower values, while IASI shows higher values over Africa, India, SE Asia and over the North Pacific, North Atlantic and Russia. These differences are likely to be the result of different resolution and sampling by the instruments (e.g. IASI and TROPOMI provide daily coverage, MOPITT takes about 3 days to provide global coverage) and the fact that the number of observations differs, e.g. about 240,000 'good'

TROPOMI data per day, compared to about 40,000 'used' MOPITT and about 60,000 used IASI observations per instrument.

Figure 5 shows analysis departures from the four datasets using the respective averaging kernels. Because MOPITT and IASI TCCO are actively assimilated in the CAMS analysis their analysis departures are small. TROPOMI is not assimilated and hence not influencing the analysis. MOPITT has negative analysis departures over Africa, SE Asia, South America and land areas in the NH, while IASI has small positive departures. TROPOMI has larger analysis departures than the other three instruments (in part because it does not influence the analysis) with negative departures in the Tropical biomass burning areas and over the Ganges valley in India and positive departures in the NH Extratropics, north of about 40ºN. These large positive departures could either point to a problem with the TROPOMI retrieval at high northern latitudes, or they could be due to a low bias of the model in those areas or both. Validation reports that are produced for the CAMS real-time system (https://atmosphere.copernicus.eu/global-services) show that CO values in the lower troposphere over Europe and in the lower and free troposphere over Asia are too low compared to IAGOS aircraft data. CAMS surface CO also shows a low bias against GAW surface observations in Europe and Asia. Therefore, part of the bias between TROPOMI TCCO and CAMS might stem from a low bias in the CAMS system that is not corrected by the MOPITT and IASI data assimilation because the TIR retrievals are mainly sensitive to CO in the mid troposphere, which is reflected in their averaging kernels and observation errors.

The positive TROPOMI departures also show up in histogram plots of departures (Fig. 6) which are skewed to high values with a mean bias of $0.17\pm0.27\ 10^{18}$ molec cm^{-2} in the NH. In the Tropics, the mean bias is smaller and negative ($-0.07\pm 0.19\ 10^{18}$ molec cm^{-2}) and in the SH the mean bias is small and positive ($0.009 \pm 0.12\ 10^{18}$ molec cm^{-2}). These biases are larger than those of the assimilated MOPITT and IASI-AB data, which are shown in Table 2, especially in the NH.

Figure 7 shows timeseries of daily area averaged TROPOMI TCCO departures and the number of daily 'good' observations from 28 January to 3 May 2018 for the Globe and five latitude bands. The figure shows that there were periods without data (especially at the beginning of March due to special calibration measurements) and changing data numbers before the middle of February. From mid-March onwards the number of observations was more stable. The satellite was still during its commissioning phase until 24 April which led to interruptions in the data availability. In the NH midlatitudes (Fig. 7c), the departures are positive and change with time, with larger departures in February and March and reducing departures from March to May. This points to a seasonally varying bias between the analysis and the data. In the Tropics (Fig. 7d) the departures are negative and again smoother after mid-March. The departures decrease from April to May. In the SH midlatitudes (Fig. 7e), the departures are small after an initial change from larger negative values and oscillate between positive and negative values. The analysis (using MOPITT and IASI) is drawing slightly away from the TROPOIM data in the SH (analysis departures greater than first-guess departures). This agrees with the negative bias seen between TROPOMI and the other instruments in the SH (Fig. 3), as assimilation of MOPITT and IASI data acts to lower the TCCO analysis and therefore increases the differences between TROPOMI and the analysis slightly.

Figure 8 shows Hovmoeller plots of TROPOMI analysis departures and numbers of observations for the period 28 January to 3 May 2018 and illustrates how the data coverage and the high analysis departures

in the NH change with time, how the largest positive analysis departures are found at the northern parts of the orbits and that negative analysis departures are found in the tropics.

Figure 9 shows scatter plots of TROPOMI TCCO analysis departures for the period 28 January to 3 May 2018 against latitude and scan angle, as well as against solar elevation separately for NH and SH. Such plots can be very useful in identifying retrieval problems depending on the chosen parameters. The scatter plot against latitude (Fig. 9a) confirms the small TCCO bias of TROPOMI against CAMS in the SH, the small negative bias in the Tropics and the larger positive bias in the NH starting at about 40ºN. The solar elevation plots (Fig. 9 c and d) show that this bias increases with increasing solar elevation in the NH but does not show a dependency on solar elevation in the SH. This suggests that the NH bias is not just a latitude bias, and that using a SOE based filter as an additional quality control might allow us to assimilate the data. Figure 9b shows that there is no obvious dependency of the analysis departures on the scan angle.

3.2 Assimilation tests with TROPOMI CO data

An assimilation experiment (ASSIM) was carried out with the TROPOMI data, where 'good' data were assimilated in the NH for solar elevations greater than 25º and for all solar elevations in the SH at latitudes north of 65ºS. The solar elevation cut-off was chosen to remove the data with the largest departures in the NH and the latitude cut-off to avoid assimilating data over the Antarctic, where the data quality is poorer. For this first assimilation test no bias correction was applied to the TROPOMI data. Further tests are required to decide which VarBC predictors to use for TROPOMI TCCO. MOPITT and IASI data were assimilated in ASSIM in the same way as in the monitoring experiment (CTRL) discussed in Section 3.1 (see also Table 1).

3.2.1 Impact of the TROPOMI assimilation

Figure 10 shows timeseries of daily global mean TROPOMI, MOPITT and IASI-AB TCCO departures, standard deviations of departures and number of observations between 28 January and 3 May 2018 for 'used data'. The figure shows that the analysis is drawing to the data and that analysis departures and their standard deviations are smaller than the first-guess ones. The global mean TROPOMI first-guess departures vary between positive and negative and the global mean analysis departures are small and positive. A small negative bias remains for MOPITT. The figure also shows that MOPITT is lower than the analysis in the global mean, while IASI-AB have positive departures that are successfully removed by the bias correction. The timeseries of the number of observations shows that considerably more observations are used per day from TROPOMI (~240,000) compared to MOPITT (~40,000) and IASI-AB (~60,000 each).

Table 3 lists mean biases and standard deviations from all four TCCO datasets for the period 28 January to 3 May 2018 from ASSIM. It shows that TROPOMI TCCO bias and standard deviation are reduced compared to CTRL (Table 2). The fit to MOPITT in the NH is degraded in ASSIM compared to CTRL, but it is improved in the Tropics and the SH. This suggests that the information added by TROPOMI to the analysis is contrary to MOPITT in the NH, while in the Tropics and SH they do not fight each other. The IASI-AB bias remains largely unchanged in the NH and Tropics and is increased in the SH. For IASI-AB the bias correction that is applied to the data can adjust to any information brought into the analysis by TROPOMI.

Figure 11 shows timeseries of area averaged daily mean TROPOMI departures and number of observations for the period 28 January to 3 May 2018 for 4 latitude bands. Figure 11a shows how the data volume at high northern latitudes increases throughout spring, and that the assimilation of TROPOMI data north of 70ºN starts at the beginning of March. Between 70-20ºN the first-guess departures are much larger until the beginning of March than during the rest of the period. This agrees with what was seen for CTRL (Fig. 7d). In the Tropics and SH, the first-guess departures are negative and the analysis departures again small.

Figure 12 shows the mean TCCO fields from CTRL and ASSIM as well as their absolute and relative differences averaged over the period 28 January to 3 May 2018. The largest impact of the TROPOMI assimilation (both in absolute and relative terms) is seen at high northern latitudes where it leads to an increase in TCCO of up to 30%. In the Tropics, including India and SE Asia, the TROPOMI assimilation reduces TCCO. The absolute changes in the SH are small as TCCO values are lower here, but the relative differences are large. It should be noted that even though no TROPOMI data are assimilated south of 65ºS there is an impact from the assimilation in the polar region. This must be due to transport of CO from the regions where the TROPOMI data are assimilated.

Figure 13 shows cross sections of zonal mean absolute and relative CO differences from ASSIM minus CTRL averaged over the period 28 January to 3 May 2018. The impact of TROPOMI is to increase CO in the Extratropical troposphere below about 300 hPa, with the largest absolute impact in the lower troposphere. CO is also increased between 200 and 100 hPa north of 60ºN. In other areas, the TROPOMI assimilation leads to a decrease of CO above about 300 hPa with the largest relative change south of 30ºS. In the Tropics, CO is reduced in the mid and upper troposphere, but absolute and relative differences are smaller than in the Extratropics. Figure 13 suggests that the impact of TROPOMI (which is sensitive to the CO column) in the CAMS analysis is largest in the lower and upper troposphere where the analysis is not already well constrained by the TIR MOPITT and IASI retrievals, which are more sensitive to the mid troposphere.

3.2.2 Validation with independent observations

To assess if the assimilation of TROPOMI CO data improves or degrades the CAMS CO analysis the CO fields from ASSIM and CTRL are compared with independent observations. We use for comparison the following datasets. (1) Column-averaged dry molar fraction CO amount (XCO) from Total Carbon Column Observing Network stations (TCCON, GGG2014 data, Wunch et al., 2011, see www.tccon.caltech.edu) at several sites (see Table 2). The absolute accuracy of the TCCON column measurements is about 4% (Wunch et al. 2010). (2) IAGOS (In-service Aircraft for a Global Observing System) vertical CO profiles from instruments mounted on commercial aircraft taken during take-off and landing. The IAGOS CO data have an accuracy of ± 5 ppbv, a precision of ± 5 % and a detection limit of 10 ppbv (Nédélec et al., 2003). (3) Ground-based data from the World Meteorological Organization's (WMO) Global Atmosphere Watch (GAW) surface observations (e.g., Oltmans and Levy, 1994; Novelli and Masarie, 2014). GAW CO data have a maximum uncertainty between ± 2 ppbv and ± 5 ppbv for marine boundary layer sites and continental sites that are influenced by regional pollution (WMO, 2010), but it has to be born in mind that the data we use in this paper are intermediate (not fully validated) near real-time data.

Comparison of XCO from ASSIM and CTRL with TCCON data is given in Fig. 14 and the mean biases and standard deviations of the biases over the period 28 January to 2 May 2018 are given in Table 3. Figure 14 and Table 3 show that the assimilation of TROPOMI CO leads to increased XCO values which means larger biases with respect to TCCON in ASSIM than in CTRL at all stations except Lauder in the SH, while the standard deviations are reduced at all stations except Sodankyla. This agrees with the sign of the TCCO departures in Fig. 13 and shows that in terms of XCO the assimilation of TROPOMI TCCO degrades the fit to the TCCON data in the NH, while improving it at Lauder in the SH. The positive bias against TCCON agrees with the findings of Borsdorff et al. (2018b) who concluded that the TROPOMI CO dataset is biased high by about 6% compared to the ground-based CO column measurements of TCCON network at nine selected sites.

Figure 15 shows comparison of CO profiles from ASSIM and CTRL with IAGOS CO profiles for six areas where there were reasonable numbers of IAGOS profiles. Over Europe (Fig. 15a), the assimilation of TROPOMI TCCO increases CO in the lower troposphere where the negative bias (below about 600 hPa) is reduced that is seen in CTRL and that is a known issue of the CAMS system. Over Japan (Fig. 15b) there is also a reduced negative bias in the lower troposphere (below 900 hPa) and an improved fit above 400 hPa, but an increased positive bias between 300-600 hPa. Over Australia and New Zealand (Fig. 15c) the TROPOMI again assimilation increases CO values below about 600 hPa and increases them above, which improves the fit to IAGOS below 600 hPa and above 300 hPa, but leads to a larger negative bias between about 300 and 500 hPa. These changes in the vertical structure were also seen in Fig. 13. Over SE Asia (Fig.15d) the mean differences between ASSIM and CTRL are small, but ASSIM is generally better than CTRL. Over India (Fig. 15e) we see an improved fit in ASSIM in the mid troposphere but a degraded fit in the lower and upper troposphere. Over West Africa (Fig. 15f) ASSIM is generally lower than CTRL which improves the fit in the mid troposphere but degrades it below about 700 hPa and above 250 hPa.

Finally, we compare the CO analysis data with six GAW surface stations (Fig. 16). At the European stations (Hohenpeissenberg, Sonnblick, Jungfraujoch, Monte Cimone) the assimilation of TROPOMI CO leads to increased surface CO analysis values and a better agreement with the GAW data than in CTRL. In particular, high CO events seen by the GAW observations are better captured in ASSIM. At Cape Verde, the assimilation of TROPOMI CO also leads to an increase of surface CO in ASSIM, but here this degrades the fit with the GAW data. At the South American station of Ushuaia, the TROPOMI assimilation again leads to increased surface CO values, which gives an overestimation of low background values, but captures better some of the higher values.

4 Conclusions

We monitored offline TROPOMI TCCO data (V1.0.2) with the CAMS system for the period 28 January to 3 May 2018. These data were mostly from the so-called S5P commissioning phase that lasted until 24 April 2018, but even these early data were good enough to test their use in the CAMS system. Overall, the data are found to be of good quality and to agree well with the CAMS CO analysis over large parts of the Globe. The data successfully capture the global TCCO distribution with high values in the NH, lower values in the SH, high values over the biomass burning areas in the Tropics and the areas of high

anthropogenic pollution over India and SE Asia, similar to MOPITT and IASI. However, there are some biases between the TROPOMI data and the CAMS CO analysis, particularly in the NH north on 40ºN where TROPOMI TCCO values are higher than CAMS. Because the CAMS system is known to underestimate CO in the NH Extratropics, particularly during winter/spring and in the lower troposphere, part of this bias is likely to be the result of a CAMS model bias. Relative to CAMS and averaged over the period from 28 January to 3 May 2018, the TROPOMI data have a positive bias of $0.17 \pm 0.27\ 10^{18}$ molec cm^{-2} in the NH, a small negative bias $-0.07 \pm 0.19\ 10^{18}$ molec cm-2 in the Tropics and a small positive bias of $0.009 \pm 0.12\ 10^{18}$ molec cm^{-2} in the SH. The bias of TROPOMI against CAMS has a dependency on latitude, with larger positive biases at low solar elevations or high latitudes in the NH. There is no noticeable dependency of the bias on scan position.

When TROPOMI data are assimilated in the CAMS system they lead to increased CO values in the Extratropics and decreased values in the Tropics. The impact of the TROPOMI assimilation is large, with TCCO changes of up to 30% at high northern latitudes, and it also has a large impact of the vertical distribution of CO in the CAMS analysis. This illustrates that the TROPOMI data, which are retrieved from the SWIR part of the solar spectrum, bring information into the CAMS system that is not already given by the other assimilated TCCO data (i.e. TIR MOPITT and IASI-AB retrievals) thanks to their different sensitivity to CO in the troposphere, especially to CO in the lower troposphere. The largest absolute and relative changes between assimilation tests with (ASSIM) and without (CTRL) the assimilation of TROPOMI TCCO are found in the lower and upper troposphere, i.e. that part of the atmosphere that is not already well constrained by the TIR MOPITT and IASI TCCO retrievals.

Relative to IAGOS CO profiles, most areas show some improved fit in ASSIM compared to CTRL. There is an improved fit to IAGOS over Europe in the lower troposphere where the negative CO bias is reduced in ASSIM. This underestimation is a known problem of the CAMS system and it is very promising to see that the TROPOMI assimilation can partially correct it. A similar improvement is also seen in the lower troposphere in the SH over Australia and New Zealand. Over India and West Africa, the assimilation of TROPOMI data leads to reduced biases in the free troposphere, but increased negative biases in the lower and upper troposphere. Over SE Asia the fit with IAGOS is also improved. However, the assimilation of TROPOMI TCCO data degrades the fit to TCCON XCO data, as it leads to larger positive biases in ASSIM than in CTRL at all stations, except at Lauder in the SH where the bias is reduced. The assimilation of TROPOMI CO leads to an improved fit with European GAW surface CO observations but to an overestimation of surface CO at Cape Verde.

The first assimilation tests presented in this paper have shown very encouraging results. More work and longer assimilation tests are needed to investigate the biases seen in comparison with the independent observations (especially TCCON) in more detail. It might be necessary to re-assess the quality control applied to the data and additional assimilation tests are needed to determine suitable bias correction predictors for TROPOMI TCCO, so that the data can be bias corrected in future experiments. It will be interesting to see how the TROPOMI biases change over the course of a year as more data become available. Also, the TROPOMI data used in this paper are the first retrieval version and it is possible that there are still issues with the data (especially with overestimation of TCCO in the NH Extratropics) and that the data quality could be improved.

The TROPOMI TCCO offline data come too late to be included in the real-time CAMS system for routine monitoring and possible assimilation. However, a near real-time TROPOMI TCCO data product is now also available and was included passively in the operational CAMS system in November 2018 to produce daily routine monitoring statistics, and the assimilation of the near real-time TROPOMI CO data in the CAMS system is being tested.

Acknowledgements

Thanks to Sebastien Massart for help with the plotting of the TCCON XCO data and to Luke Jones with the IAGOS and GAW validation. Thanks to the data providers of the data assimilated in the CAMS reanalysis and the data used for the validation studies in this paper. The Copernicus Atmosphere Monitoring Service is operated by the European Centre for Medium-Range Weather Forecasts on behalf of the European Commission as part of the Copernicus programme (http://copernicus.eu). TB acknowledges funding by the TROPOMI national program from NSO. The TROPOMI data processing was carried out on the Dutch national e-infrastructure with the support of the SURF cooperation.

References

Benedetti, A., Morcrette, J.-J., Boucher, O., Dethof, A., Engelen, R. J., Fisher, M., Flentje, H., Huneeus, N., Jones, L., Kaiser, J. W., Kinne, S., Mangold, A., Razinger, M., Simmons, A. J., Suttie, M., and the GEMS-AER team: Aerosol analysis and forecast in the European Centre for Medium-Range Weather Forecasts Integrated Forecast System: Data Assimilation. J. Geophys. Res., D13205, 114, doi:10.1020/2008JD011115, 2009.

Borsdorff, T., Aan de Brugh, J., Hu, H., Aben, I., Hasekamp, O., and Landgraf, J.: Measuring carbon monoxide with TROPOMI: First results and a comparison with ECMWF-IFS analysis data. Geophysical Research Letters, 45, 2826–2832. https://doi.org/10.1002/2018GL077045, 2018.

T. Borsdorff, J. aan de Brugh, H. Hu, O. Hasekamp, R. Sussmann, M. Rettinger, F. Hase, J. Gross, M. Schneider, O. Garcia, W. Stremme, M. Grutter, D. G. Feist, S. G. Arnold, M. De Mazière, M. Kumar Sha, D. F. Pollard, M. Kiel, C. Roehl, P. O. Wennberg, G. C. Toon, and Landgraf, J.: Mapping carbon monoxide pollution from space down to city scales with daily global coverage. Atmospheric Measurement Techniques Discussions, 2018:1–19, 2018.

Clerbaux, C., Boynard, A., Clarisse, L., George, M., Hadji-Lazaro, J., Herbin, H., Hurtmans, D., Pommier, M., Razavi, A., Turquety, S., Wespes, C., and Coheur, P.-F.: Monitoring of atmospheric composition using the thermal infrared IASI/MetOp sounder, Atmos. Chem. Phys., 9, 6041-6054, 2009.

Courtier, P., Thépaut, J.-N. and Hollingsworth, A.: A strategy for operational implementation of 4D-Var, using an incremental approach. Q. J. R. Meteorol. Soc., 120, 1367-1388, 1994.

Dee, D. P. and Uppala, S.: Variational bias correction of satellite radiance data in the ERA-Interim reanalysis. Q. J. R. Meteorol. Soc, 135, 1830–1841, 2009.

Deeter, M. N., Edwards, D. P., Francis, G. L., Gille, J. C., Martínez-Alonso, S., Worden, H. M., and Sweeney, C.: A climate-scale satellite record for carbon monoxide: the MOPITT Version 7 product, Atmos. Meas. Tech., 10, 2533-2555, https://doi.org/10.5194/amt-10-2533-2017, 2017.

Deeter, M. N., Martínez-Alonso, S., Edwards, D. P., Emmons, L. K., Gille, J. C. , Worden, H. M., Pittman, J. V., Daube, B. C., and Wofsy, S. C.: Validation of MOPITT Version 5 thermal-infrared, near-infrared, and multispectral carbon monoxide profile retrievals for 2000–2011, J. Geophys. Res. Atmos., 118, 6710–6725, doi:10.1002/jgrd.50272, 2013.

Flemming, J., Benedetti, A., Inness, A., Engelen, R. J., Jones, L., Huijnen, V., Remy, S., Parrington, M., Suttie, M., Bozzo, A., Peuch, V.-H., Akritidis, D., and Katragkou, E.: The CAMS interim Reanalysis of Carbon Monoxide, Ozone and Aerosol for 2003–2015, Atmos. Chem. Phys., 17, 1945-1983, https://doi.org/10.5194/acp-17-1945-2017, 2017.

Flemming, J., Huijnen, V., Arteta, J., Bechtold, P., Beljaars, A., Blechschmidt, A.-M., Diamantakis, M., Engelen, R. J., Gaudel, A., Inness, A., Jones, L., Josse, B., Katragkou, E., Marecal, V., Peuch, V.-H., Richter, A., Schultz, M. G., Stein, O., and Tsikerdekis, A.: Tropospheric chemistry in the Integrated Forecasting System of ECMWF, Geosci. Model Dev., 8, 975-1003, doi:10.5194/gmd-8-975-2015, 2015.

George, M., Clerbaux, C., Hurtmans, D., Turquety, S., Coheur, P.-F., Pommier, M., Hadji-Lazaro, J., Edwards, D. P., Worden, H., Luo, M., Rinsland, C., and McMillan, W.: Carbon monoxide distributions from the IASI/METOP mission: evaluation with other space-borne remote sensors. Atmos. Chem. Phys., 9, 8317–8330, 2009.

George, M., Clerbaux, C., Bouarar, I., Coheur, P.-F., Deeter, M. N., Edwards, D. P., Francis, G., Gille, J. C., Hadji-Lazaro, J., Hurtmans, D., Inness, A., Mao, D., and Worden, H. M.: An examination of the long-term CO records from MOPITT and IASI: comparison of retrieval methodology, Atmos. Meas. Tech., 8, 4313-4328, https://doi.org/10.5194/amt-8-4313-2015, 2015.

Granier, C., Bessagnet, B., Bond, T., D'Angiola, A., Denier van der Gon, H., Frost, G. J., Heil, A., Kaiser, J. W., Kinne, S., Klimont, Z., Kloster,S., Lamarque, J.-F., Liousse, C., Masui, T., Meleux, F., Mieville, A., Ohara, R., Raut, J.-C., Riahi, K., Schultz, M. G., Smith, S. G., Thompson, A., van Aardenne, J., van der Werf, G. R., and van Vuuren, D. P.: Evolution of anthropogenic and biomass burning emissions of air pollutants at global and regional scales during the 1980-2010 period. Climatic Change, 109, 163-190. DOI: 10.1007/s 10584-011-0154-1, 2011.

Guenther, A., Karl, T., Harley, P., Wiedinmyer, C., Palmer, P. I., and Geron, C.: Estimates of global terrestrial isoprene emissions using MEGAN (Model of Emissions of Gases and Aerosols from Nature), Atmos. Chem. Phys., 6, 3181–3210, doi:10.5194/acp-6- 3181-2006, 2006.

Hase, F., T. Blumenstock, S. Dohe, J. Groß, Kiel, M.: TCCON data from Karlsruhe, Germany, Release GGG2014R0. TCCON data archive, hosted by the Carbon Dioxide Information Analysis Center, Oak Ridge National Laboratory, Oak Ridge, Tennessee, U.S.A. http://dx.doi.org/10.14291/tccon.ggg2014.karlsruhe01.R1/1182416, 2014.

Huijnen, V., Williams, J., van Weele, M., van Noije, T., Krol, M., Dentener, F., Segers, A., Houweling, S., Peters, W., de Laat, J., Boersma, F., Bergamaschi, P., van Velthoven, P., Le Sager, P., Eskes, H., Alkemade, F., Scheele, R., Nédélec, P., and Pätz, H.-W.: The global chemistry transport model TM5: description and evaluation of the tropospheric chemistry version 3.0, Geosci. Model Dev., 3, 445-473, doi:10.5194/gmd-3-445-2010.

Inness, A., Blechschmidt, A.-M., Bouarar, I., Chabrillat, S., Crepulja, M., Engelen, R. J., Eskes, H., Flemming, J., Gaudel, A., Hendrick, F., Huijnen, V., Jones, L., Kapsomenakis, J., Katragkou, E., Keppens, A., Langerock, B., de Mazière, M., Melas, D., Parrington, M., Peuch, V. H., Razinger, M., Richter, A., Schultz, M. G., Suttie, M., Thouret, V., Vrekoussis, M., Wagner, A., and Zerefos, C.: Data assimilation of satellite-retrieved ozone, carbon monoxide and nitrogen dioxide with ECMWF's Composition-IFS, Atmos. Chem. Phys., 15, 5275-5303, doi:10.5194/acp-15-5275-2015, 2015.

Inness, A., Baier, F., Benedetti, A., Bouarar, I., Chabrillat, S., Clark, H., Clerbaux, C., Coheur, P., Engelen, R. J., Errera, Q., Flemming, J., George, M., Granier, C., Hadji-Lazaro, J., Huijnen, V., Hurtmans, D., Jones, L., Kaiser, J. W., Kapsomenakis, J., Lefever, K., Leitão, J., Razinger, M., Richter, A., Schultz, M. G., Simmons, A. J., Suttie, M., Stein, O., Thépaut, J.-N., Thouret, V., Vrekoussis, M., Zerefos, C., and the MACC team: The MACC reanalysis: an 8 yr data set of atmospheric composition, Atmos. Chem. Phys., 13, 4073-4109, doi:10.5194/acp-13-4073-2013, 2013.

Kaiser, J. W., Heil, A., Andreae, M. O., Benedetti, A., Chubarova, N., Jones, L., Morcrette, J.-J., Razinger, M., Schultz, M. G., Suttie, M., and van der Werf, G. R.: Biomass burning emissions estimated with a global fire assimilation system based on observed fire radiative power. Biogeosciences, 9:527–554, 2012.

Kivi, R., P. Heikkinen, and Kyro, E.: TCCON data from Sodankyla, Finland, Release GGG2014R0. TCCON data archive, hosted by CaltechDATA, California Institute of Technology, Pasadena, CA, U.S.A. https://doi.org/10.14291/tccon.ggg2014.sodankyla01.R0/1149280, 2017.

Landgraf, J., aan de Brugh, J., Scheepmaker, R., Borsdorff, T., Hu, H., Houweling, S., Butz, A., Aben, I., and Hasekamp, O.: Carbon monoxide total column retrievals from TROPOMI shortwave infrared measurements, Atmos. Meas. Tech., 9, 4955-4975, https://doi.org/10.5194/amt-9-4955-2016, 2016.

Nedelec, P., Cammas, J.-P., Thouret, V., Athier, G., Cousin, J.-M., Legrand, C., Abonnel, C., Lecoeur, F., Cayez, G., and Marizy, C.: An improved infrared carbon monoxide analyser for routine measurements aboard commercial aircraft: technical validation and first scientific results for the MOZAIC III programme, Atmos. Chem. Phys., 3, 1551-1564, 2003.

Novelli, P.C. and Masarie, K.A.: Atmospheric Carbon Monoxide Dry Air Mole Fractions from the NOAA ESRL Carbon Cycle Cooperative Global Air Sampling Network, 1988-2013, Version: 2014-07-02, ftp://aftp.cmdl.noaa.gov/data/trace_gases/co/flask/surface/ (last access December 2014), 2014.

Oltmans, SJ and Levy II, H: Surface ozone measurements from a global network, Atmos. Environ., 28, 9-24, 1994.

Veefkind, J. P., Aben, I., McMullan, K., Förster, H., de Vries, J., Otter, G.; Claas, J., Eskes, H. J., de Haan, J. F., Kleipool, Q., van Weele, M., Hasekamp, O., Hoogeveen, R., Landgraf, J., Snel, R., Tol, P., Ingmann, P., Voors, R., Kruizinga, B., Vink, R., Visser, H., and Levelt, P. F.: TROPOMI on the ESA Sentinel-5 Precursor : A GMES Mission for global observations of the atmospheric composition for climate, air quality and ozone layer applications, remote Sensing of Environment, 120:70-83, doi:10.1016/j.rse.2011.09.027, 2012.

Sherlock, V., B. Connor, J. Robinson, H. Shiona, D. Smale, and Pollard, D.: TCCON data from Lauder, New Zealand, 120HR, Release GGG2014R0. TCCON data archive, hosted by CaltechDATA, California Institute of Technology, Pasadena, CA, U.S.A. https://doi.org/10.14291/tccon.ggg2014.lauder01.R0/1149293, 2014.

J. Vidot, J. Landgraf, O. Hasekamp, A. Butz, A. Galli, P. Tol, and Aben, I.: Carbon monoxide from shortwave infrared reflectance measurements: A new retrieval approach for clear sky and partially cloudy atmospheres. Remote Sensing of Environment, 120:255–266, 2012.

Wennberg, P. O., C. Roehl, D. Wunch, G. C. Toon, J.-F. Blavier, R. Washenfelder, G. Keppel-Aleks, N. Allen and Ayers, J.: TCCON data from Park Falls, Wisconsin, USA, Release GGG2014R1. TCCON data archive, hosted by CaltechDATA, California Institute of Technology, Pasadena, CA, U.S.A. http://doi.org/10.14291/tccon.ggg2014.parkfalls01.R1, 2017a.

Wennberg, P. O., Wunch, D., Roehl, C. M., Blavier, J.-F., Toon, G. C. and Allen, N. T.: TCCON data from Lamont (US), Release GGG2014.R1 [Data set]. CaltechDATA. https://doi.org/10.14291/tccon.ggg2014.lamont01.r1/1255070, 2017b.

Wunch, D., G. C. Toon, J.-F. L. Blavier, R. A. Washenfelder, J. Notholt, B. J. Connor, D. W. T. Griffith, V. Sherlock, and Wennberg, P. O.: The Total Carbon Column Observing Network, doi: 10.1098/rsta.2010.0240 Phil. Trans. R. Soc. A 28 May 2011 vol. 369 no. 1943 2087-2112, 2011.

Wunch, D., Toon, G. C., Wennberg, P. O., Wofsy, S. C., Stephens, B. B., Fischer, M. L., Uchino, O., Abshire, J. B., Bernath, P., Biraud, S. C., Blavier, J.-F. L., Boone, C., Bowman, K. P., Browell, E. V., Campos, T., Connor, B. J., Daube, B. C., Deutscher, N. M., Diao, M., Elkins, J. W., Gerbig, C., Gottlieb, E., Griffith, D. W. T., Hurst, D. F., Jiménez, R., Keppel-Aleks, G., Kort, E. A., Macatangay, R., Machida, T., Matsueda, H., Moore, F., Morino, I., Park, S., Robinson, J., Roehl, C. M., Sawa, Y., Sherlock, V., Sweeney, C., Tanaka, T., and Zondlo, M. A.: Calibration of the Total Carbon Column Observing Network using aircraft profile data, Atmos. Meas. Tech., 3, 1351-1362, https://doi.org/10.5194/amt-3-1351-2010, 2010.

Table 1: TCCO satellite retrievals used in this paper. QR= quality flag given by data providers, LAT: Latitude, VarBC: Variational bias correction. The blacklist criteria describe when data were not used.

Instrument/ Satellite	Overpass time	Spectral retrieval window	Data provider/ version	Blacklist criteria/ thinning criteria	VarBC predictors	Reference
MOPITT/ **Terra**	10:30	TIR(4.7µm)	NCAR, V7 (TIR)	|LAT|<65º; QR>0; Night time data over Greenland; Data not used because of instrument calibration activities between 13 February and 9 April 2018. Thinned to 0.5ºx0.5º	No VarBC applied	Deeter et al. (2017)
IASI/ **Metop-A & Metop-B**	9:30	2143−2181.25 cm^{-1} Wavenumber IASI covers 3.62-15.5µm	LATMOS/ ULB	|LAT|> 65º; QR>0; Night time data Thinned to 0.5ºx0.5º	global constant, 1000-300 hPa thickness, thermal contrast, i.e. difference between surface temperature and temperature of lowest model level	George et al. (2009), Clerbaux et al. (2009)
TROPOMI/ **S5p**	13:30	SWIR (2324-2338 nm)	SRON/ESA	LAT> 65ºS; SOE>25º for lat>0º QR>0 Super-obbed to T511	No VarBC applied	Landgraf et al. (2016)

Table 2: Mean bias and standard deviations of the TCCO retrievals against the CAMS CO analysis in 10^{18} molec/cm^2 from the control experiment (CTRL) for the period 28 January to 3 May 2018.

Instrument	NH (20-90^{0}N)	Tropics (20^{0}S-20^{0}N)	SH (20-90^{0}S)
TROPOMI (good data)	0.17±0.27	-0.68e-1±0.19	0.90e-2±0.119
MOPITT (used data)	-0.26e-1±01.42	-0.13e-1±0.132	0.86e-2±0.82e-1
IASI-A (used data)	0.11e-1±0.143	0.11e-1±0.111	0.22e-2±0.53e-1
IASI-B (used data)	0.15e-1±0.138	0.13e-1±0.112	0.39e-3±0.53e-1

Table3: Mean bias and standard deviations of the TCCO retrievals against the CAMS CO analysis in 10^{18} molec/cm^2 from the assimilation experiment (ASSIM) for the period 28 January to 3 May 2018.

Instrument	NH (20-90^{0}N)	Tropics (20^{0}S-20^{0}N)	SH (20-90^{0}S)
TROPOMI (used data)	0.29e-1±0.191	-0.82e-3±0.145	-0.84e-2±0.102
MOPITT (used data)	-0.46e-1±0.15	-0.97e-2±0.132	0.75e-2±0.83e-1
IASI-A (used data)	0.11e-1±0.147	0.12e-1±0.114	0.45e-2±0.58e-1
IASI-B (used data)	0.15e-1±0.142	0.14e-1±0.115	0.25e-2±0.58e-1

Table 4: TCCON stations used in this paper and mean biases and standard deviations from CTRL and ASSIM in ppb for the period 28 January to 2 May 2018.

Station	**Latitude, longitude**	**Reference**	**CTRL** **Bias ± stdv**	**ASSIM** **Bias ± stdv**
Sodankyla	67.37N, 26.63E	Kivi et al. (2017)	-3.57 ± 4.20	7.82 ± 4.27
Karlsruhe	49.1N,8.44E	Hase et al. (2014)	3.22 ± 6.16	6.38 ± 3.37
Parkfalls	45.94N, 90.27W	Wennberg et al. (2017a)	0.37 ± 4.38	8.03 ± 3.65
Lamont	36.6N,97.49W	Wennberg et al. (2017b)	5.52 ± 3.72	7.90 ± 2.55
Lauder	45.04S, 169.68E	Sherlock et al. (2014)	3.08 ± 1.44	2.90 ± 1.20

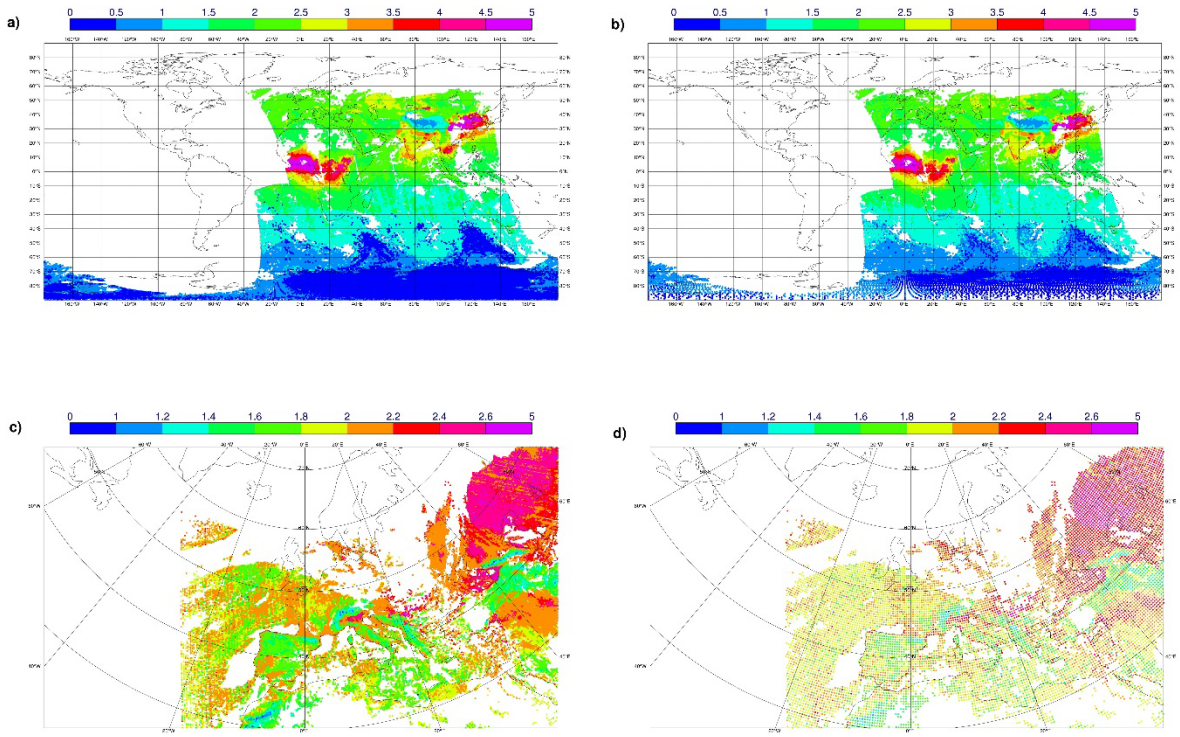

Figure 1: TROPOMI TCCO on 20180128, 12 z in 10^{18} molec/cm^2 at full resolution for (a) the Globe and (c) Europe and super-obbed to the model resolution of T511 for (b) the Globe and (d) Europe. Note that different colour scales are used for the global and European plots.

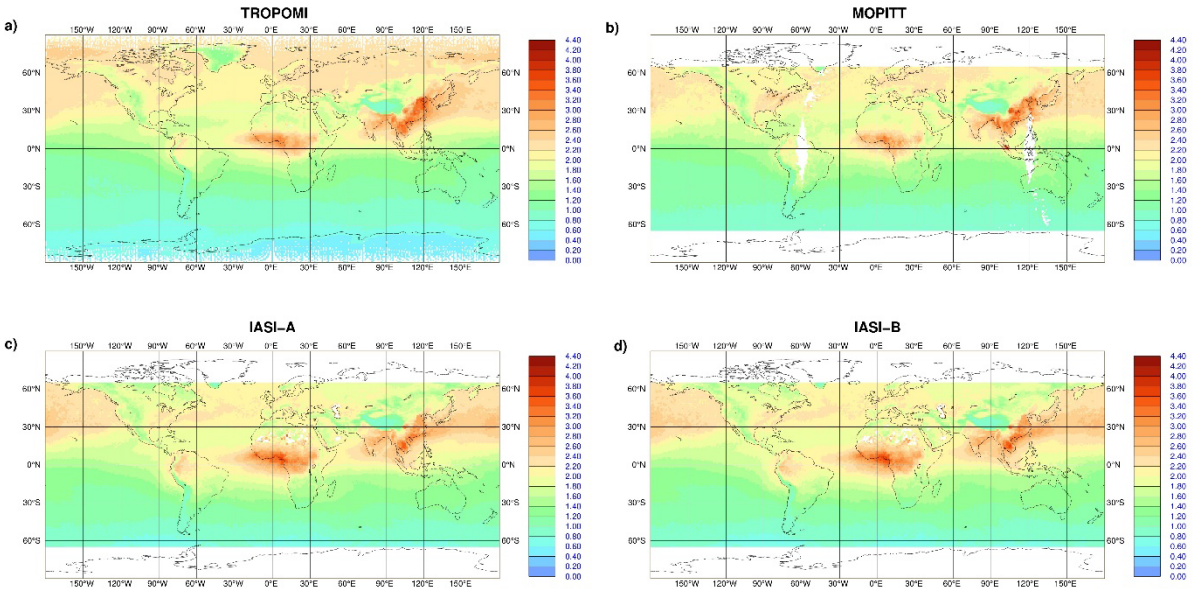

Figure 2: Mean TCCO values averaged over the period 28 January to 3 May 2018 from (a) TROPOMI, (b) MOPITT, (c) IASI-A and (d) IASI-B in 10^{18} molec cm^{-2}. For TROPOMI 'good' data are shown while for the other instruments 'used' data are shown.

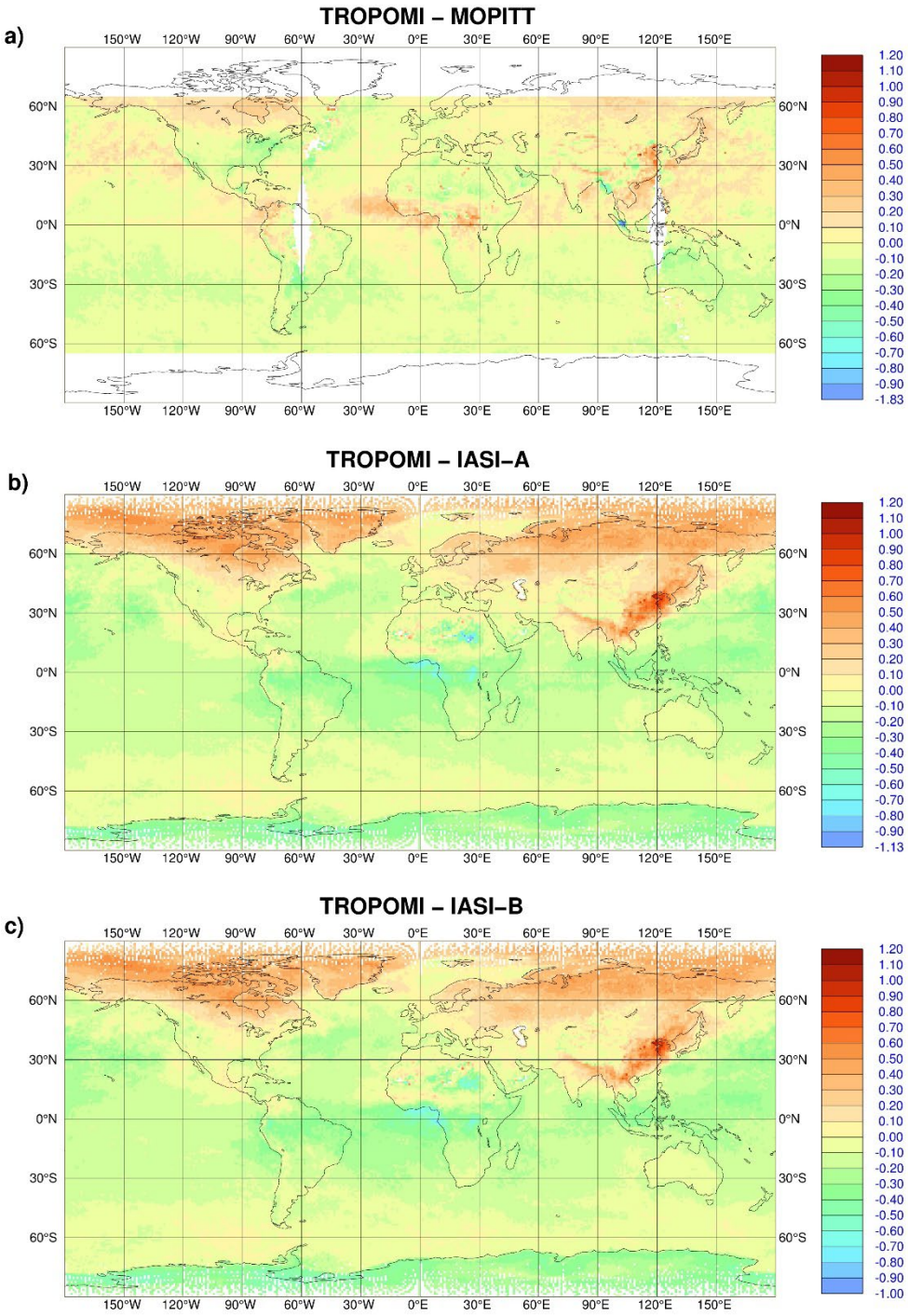

Figure 3: Mean TCCO differences averaged over the period 28 January to 3 May 2018 from (a) TROPOMI minus MOPITT, (b) TROPOMI minus IASI-A and (c) TROPOMI - IASI-B in 10^{18} molec cm^{-2}. Shown are 'good' data.

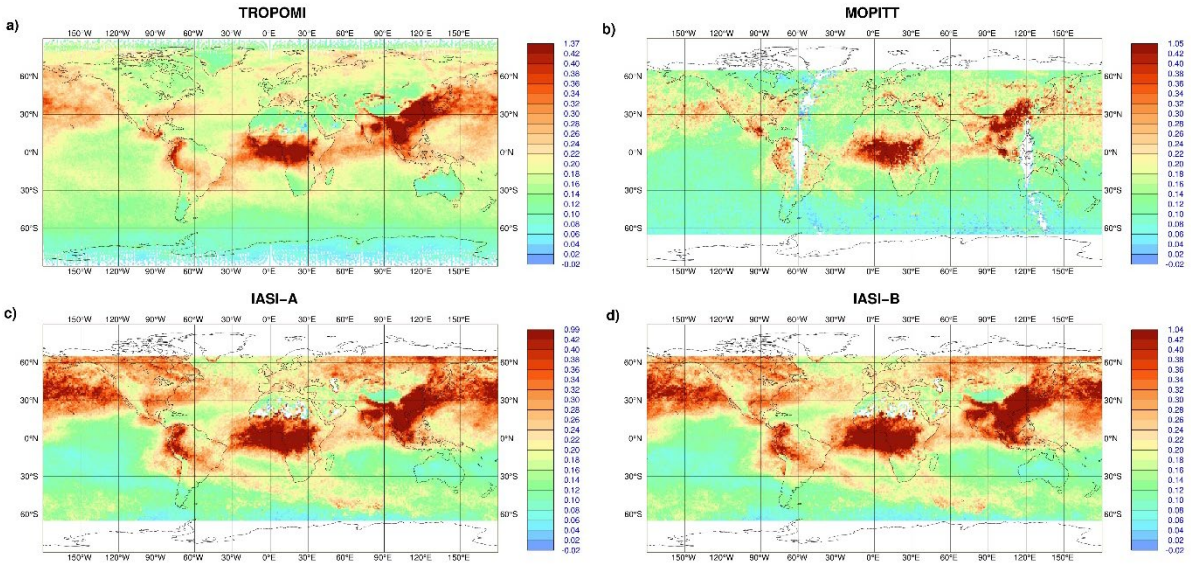

Figure 4: TCCO standard deviation for the period 28 January to 3 May 2018 from (a) TROPOMI, (b) MOPITT, (c) IASI-A and (d) IASI-B in 10^{18} molec cm^{-2}. For TROPOMI 'good' data are shown while for the other instruments 'used' data are shown.

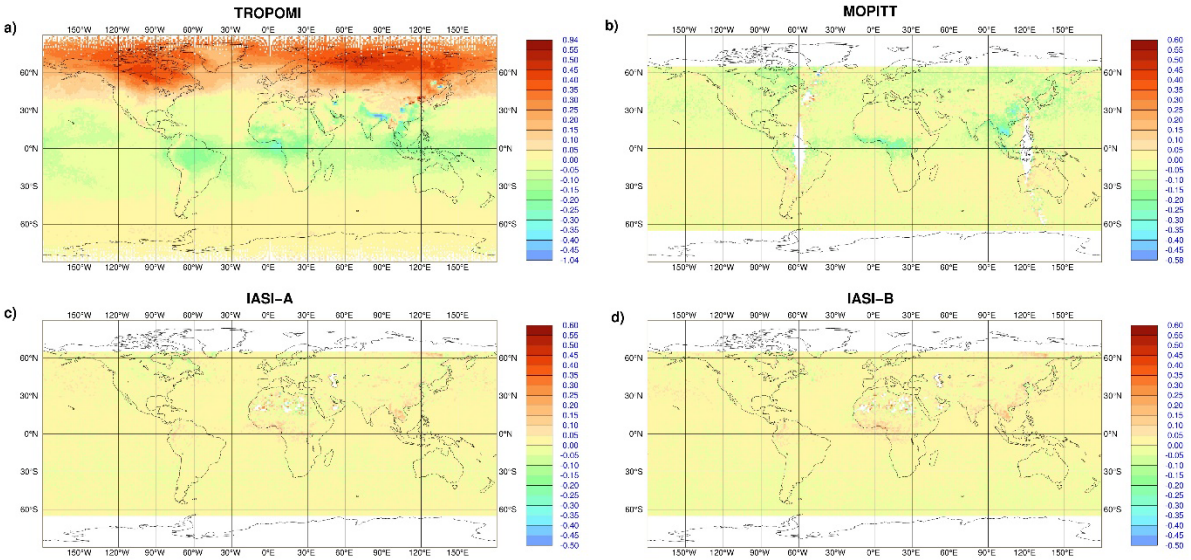

Figure 5: Mean TCCO analysis departures (observations minus analysis) averaged over the period 28 January to 3 May 2018 from (a) TROPOM, (b) MOPITT, (c) IASI-A and (d) IASI-B in 10^{18} molec cm^{-2}. For TROPOMI 'good' data are shown while for the other instruments 'used' data are shown.

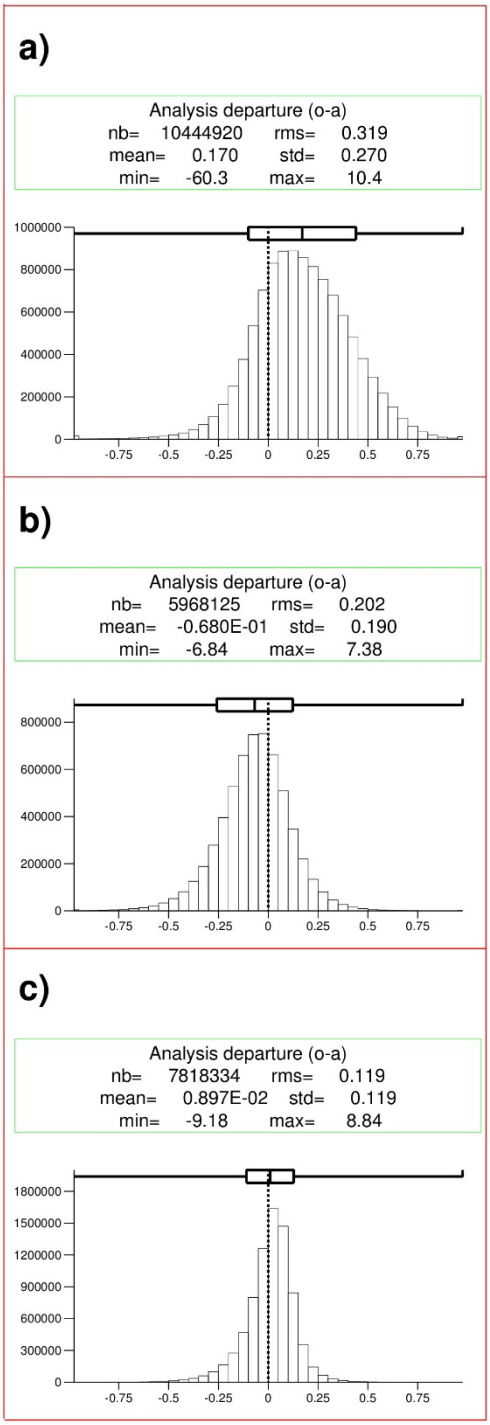

Figure 6: Histograms of TROPOMI TCCO analysis departures for the (a) NH Extratropics, (b) Tropics and (c) SH Extratropics in 10^{18} molec cm^{-2} for the period from 28 January to 3 May 2018. Shown are 'good' data.

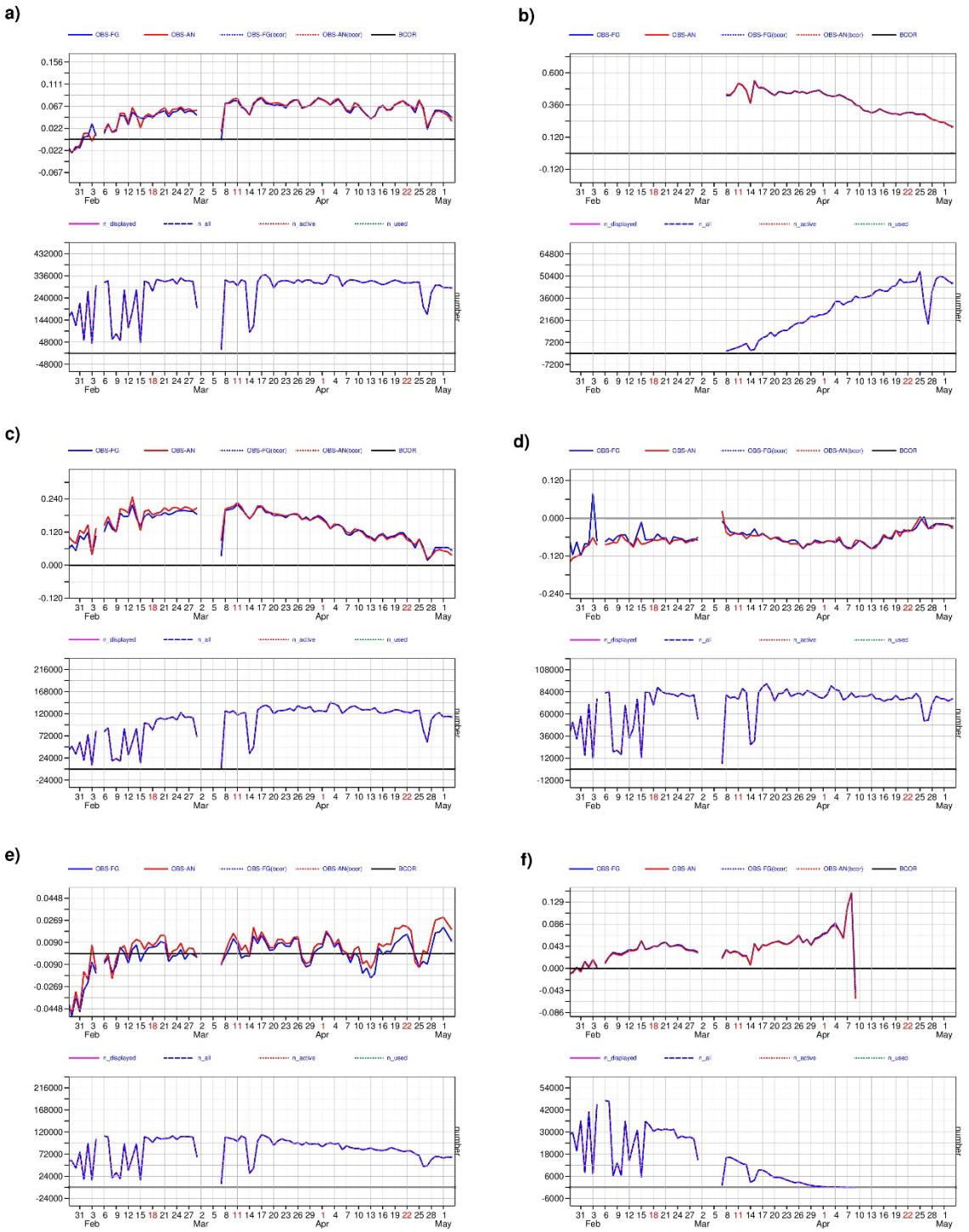

Figure 7: Time series of mean first-guess and analysis departures (top panels) in 10^{18} molec cm^{-2} and number of data (bottom panels) from TROPOMI averaged over the areas (a) 90ºN-90ºS, (b) 90ºN-70ºN, (c) 70ºN-20ºN, (d) 20ºN-20ºS, (e) 20ºS-70ºS and (f) 70ºS-90ºS. Shown are 'good' data.

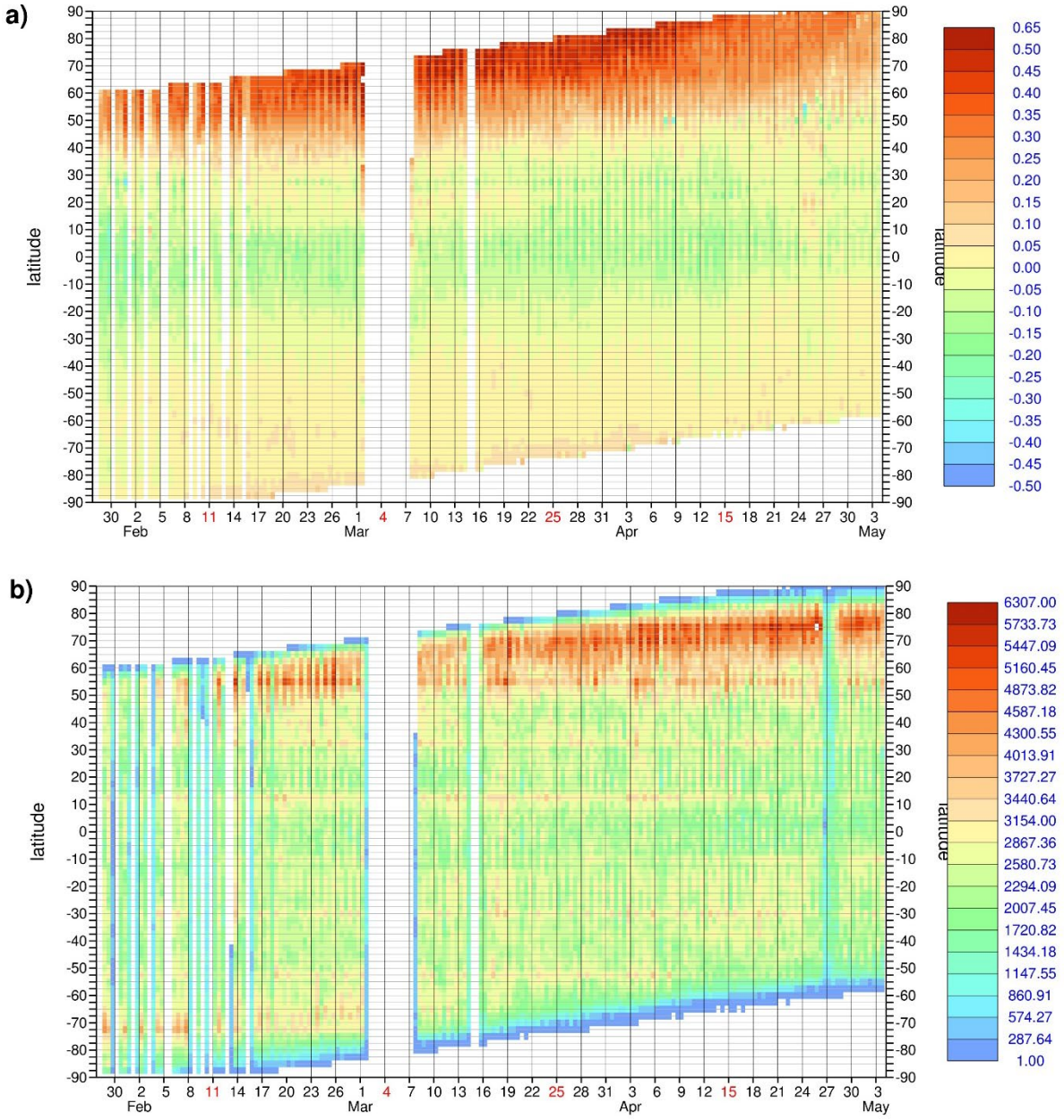

Figure 8: Hovemoeller plots (zonal mean timeseries) of (a) TROPOMI analysis departures in 10^{18} molec cm^{-2} and (b) number of observations for the period 28 January to 3 May 2018. Shown are 'good' data.

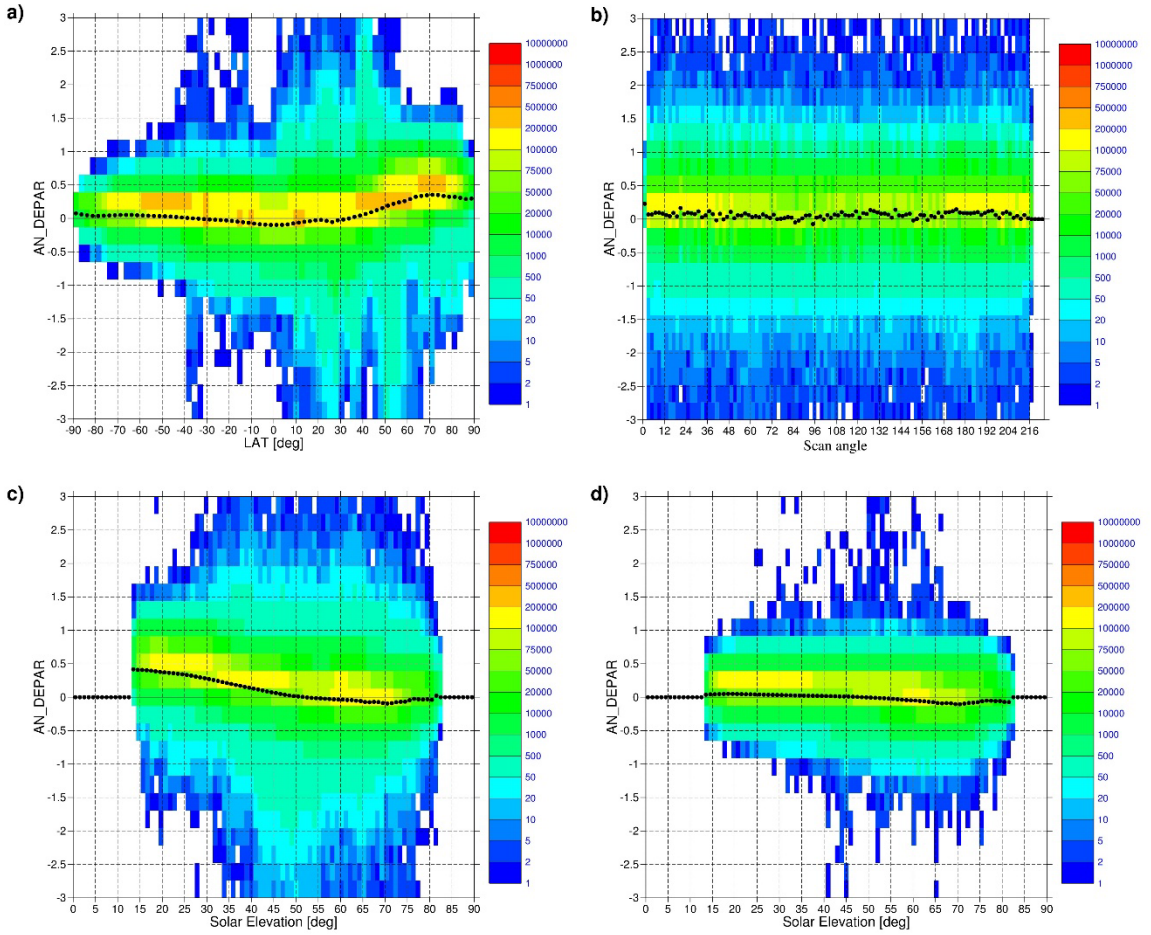

Figure 9: Scatter plots of 'good' TROPOMI TCCO analysis departures against (a) latitude, (b) scan angle, (c) solar elevation for NH data and (d) solar elevation for SH data. Values are in 10^{18} molec cm^{-2} for the period 28 January to 3 May 2018.

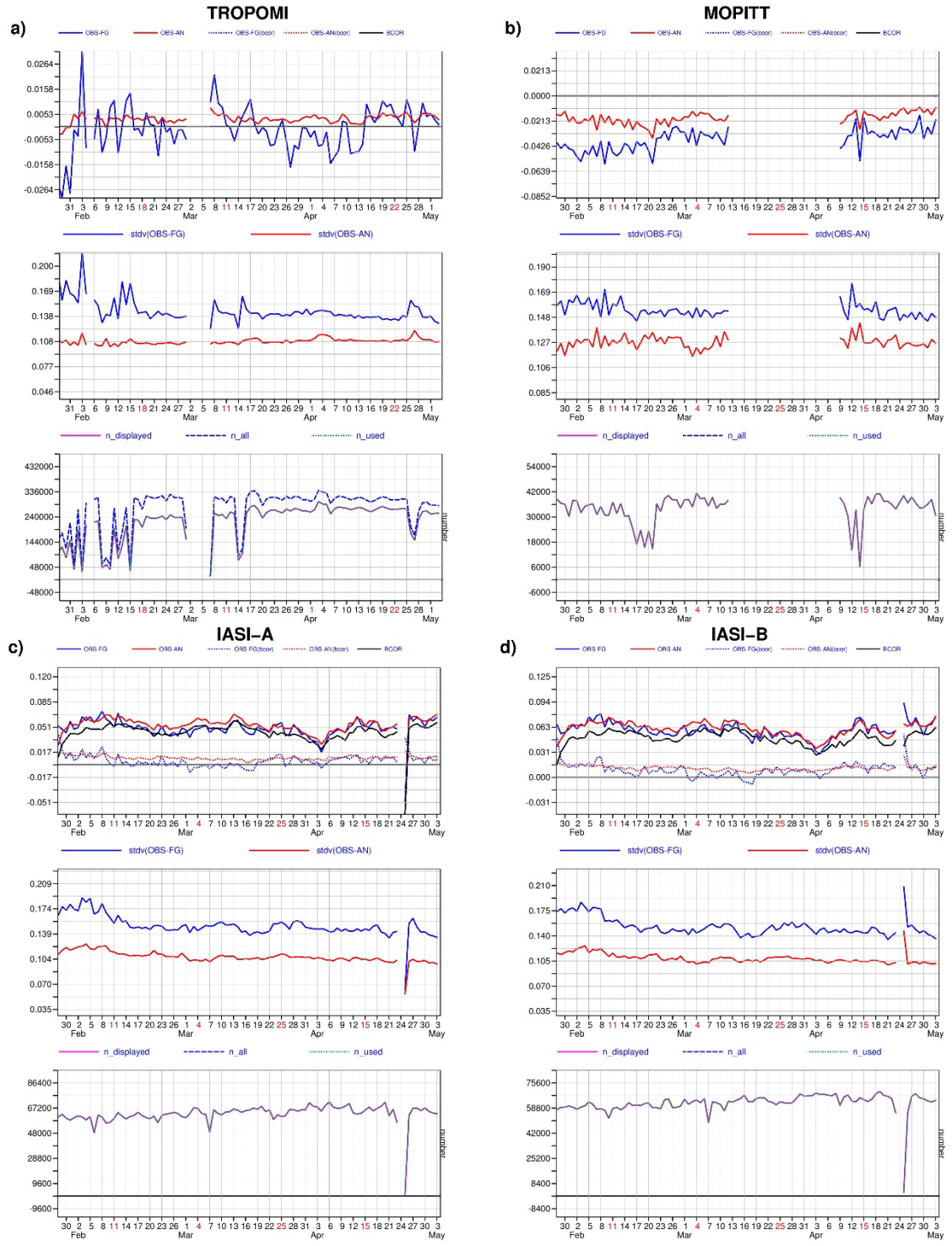

Figure 10: The top panels show time series of daily global mean first-guess departures (blue solid lines), analysis departures (red solid line, bias correction (black lines) and bias corrected analysis and first-guess departures (blue and red dotted lines), the middle panels the standard deviations of the departures in 10^{18} molec cm^{-2} and the bottom panels the number of used observations for (a) TROPOMI, (b) MOPITT, (c) IASI-A and (d) IASI-B for the period 28 January to 3 May 2018. Shown are 'used data.

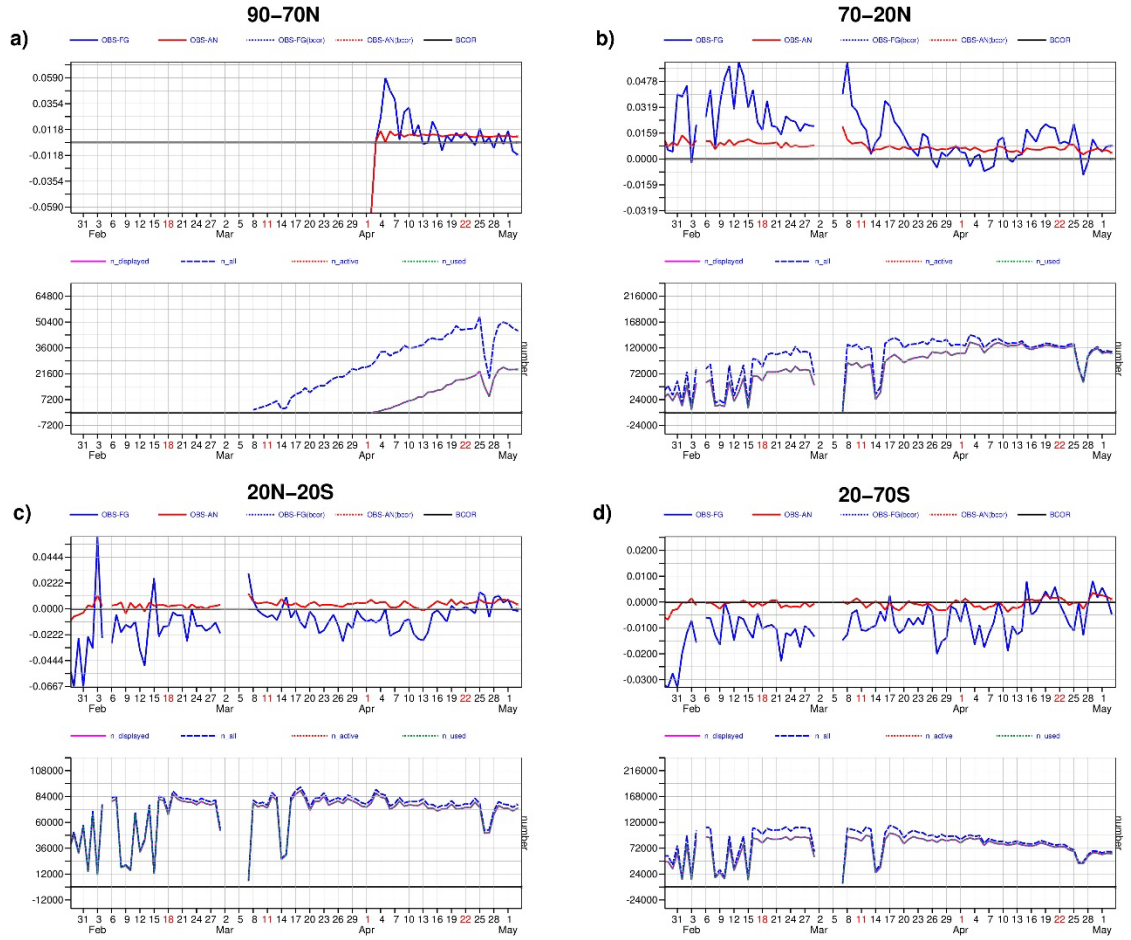

Figure 11: The top panels show time series of daily area averaged first-guess departures (blue solid lines), analysis departures (red solid line and bias correction (black lines) in 10^{18} molec cm^{-2} and the bottom panels the number of used observations from TROPOMI for the areas 90º-70ºN (a), 70º-20ºN (b), 20ºN-20ºS (c) and 20ºS-70ºS for the period 28 January to 3 May 2018. Shown are 'used data.

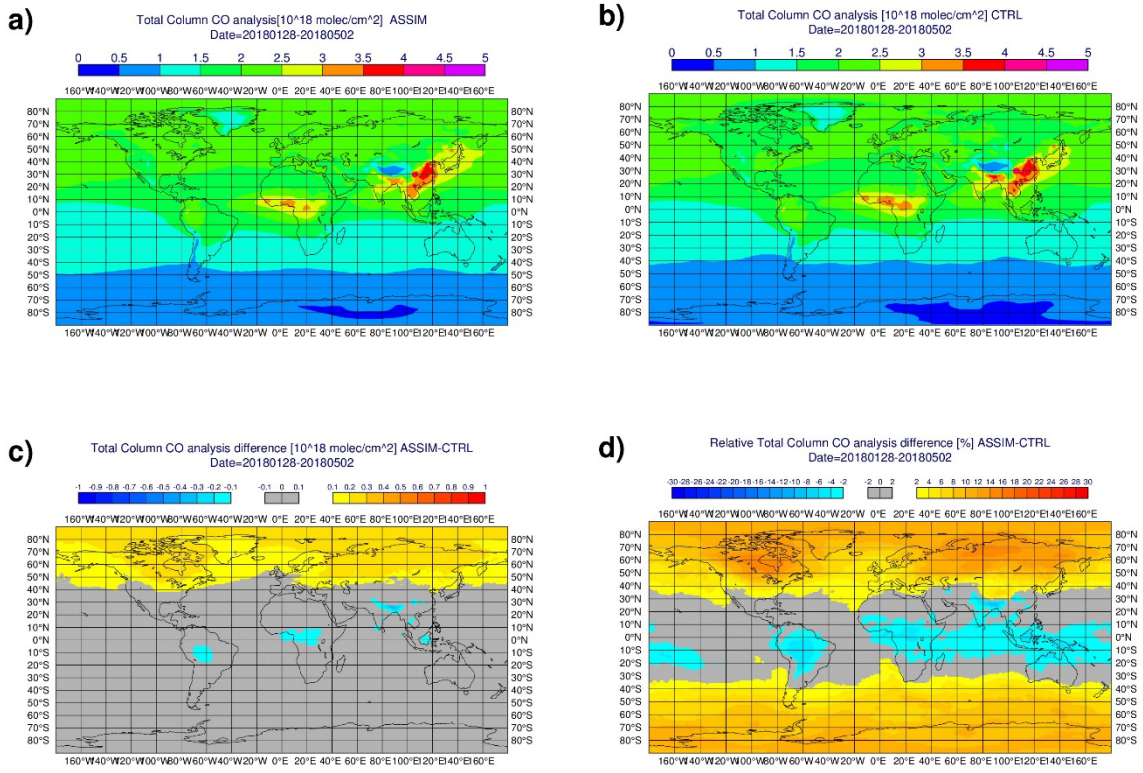

Figure 12: Mean TCCO analysis from (a) ASSIM, (b) CTRL, as well as (c) the absolute difference in 10^{18} molec cm^{-2} and (d) the relative difference in % for the period 28 January to 3 May 2018.

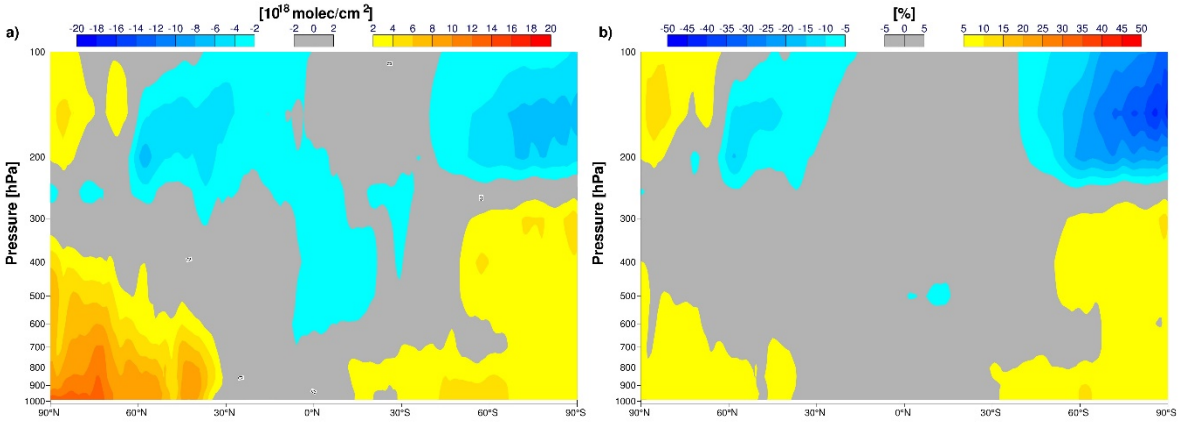

Figure 13: Cross sections of zonal mean differences from ASSIM minus CTRL averaged over the period 28 January to 3 May 2018. Shown are (a) absolute differences in parts per billion (ppb) and (b) relative differences in %.

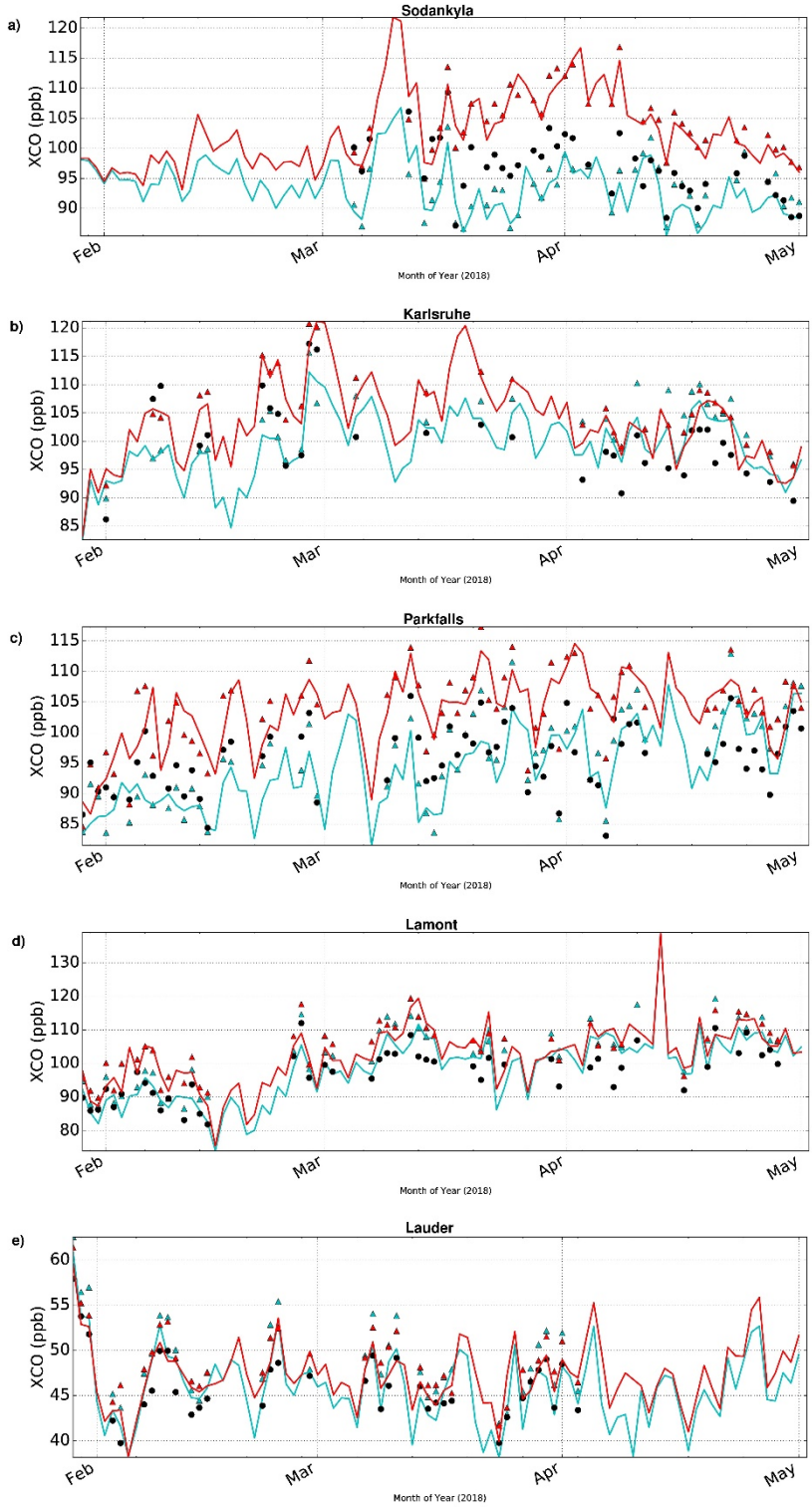

Figure 14: Column average CO (XCO) in ppb at several TCCON stations. Daily mean observations are shown by the black dots, corresponding daily mean XCO columns calculated using the TCCON averaging kernels are shows by the red (ASSIM) and blue (CTRL) triangles. The continuous lines are the daily XCO for ASSIM (red) and CTRL (blue). Show are data for (a) Sodankyla, (b) Karsruhe, (c) Parkfalls, (d) Lamont and (e) Lauder. For more information about the TCCON stations see Table 4.

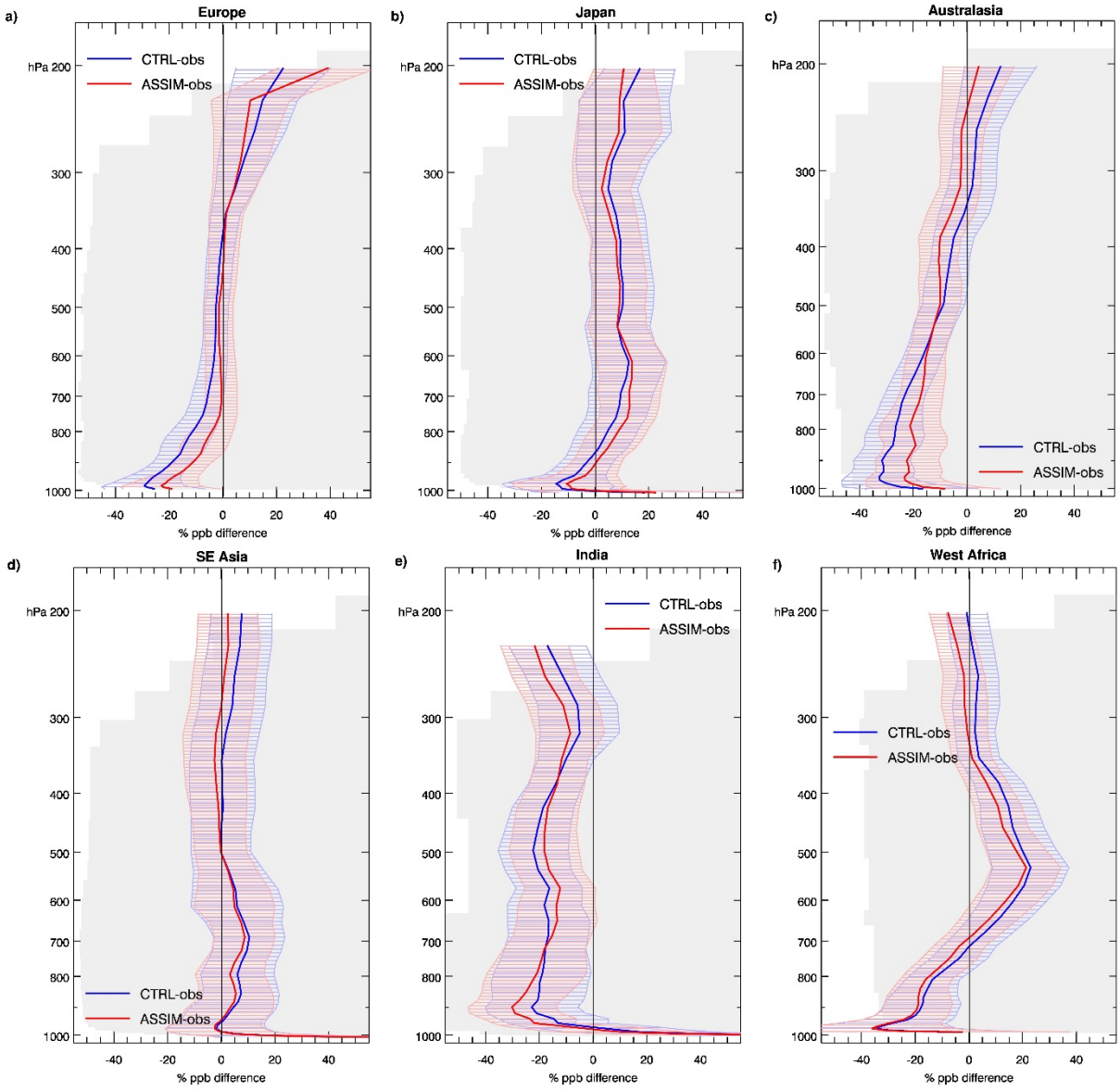

Figure 15: Mean relative CO difference in % of ASSIM minus IAGOS aircraft data (red) and CTRL minus IAGOS (blue) for the 3 months February to April 2018 for (a) Europe (3 sites, 99 profiles), (b) Japan (4 sites, 76 profiles), (c) Australia and New Zealand (4 sites, 54 profiles, (d) SE Asia (14 sites, 447 profiles), (e) India (3 sites, 26 profiles) and (f) West Africa (16 sites, 74 profiles). The shaded area shows the standard deviation of the biases over the period.

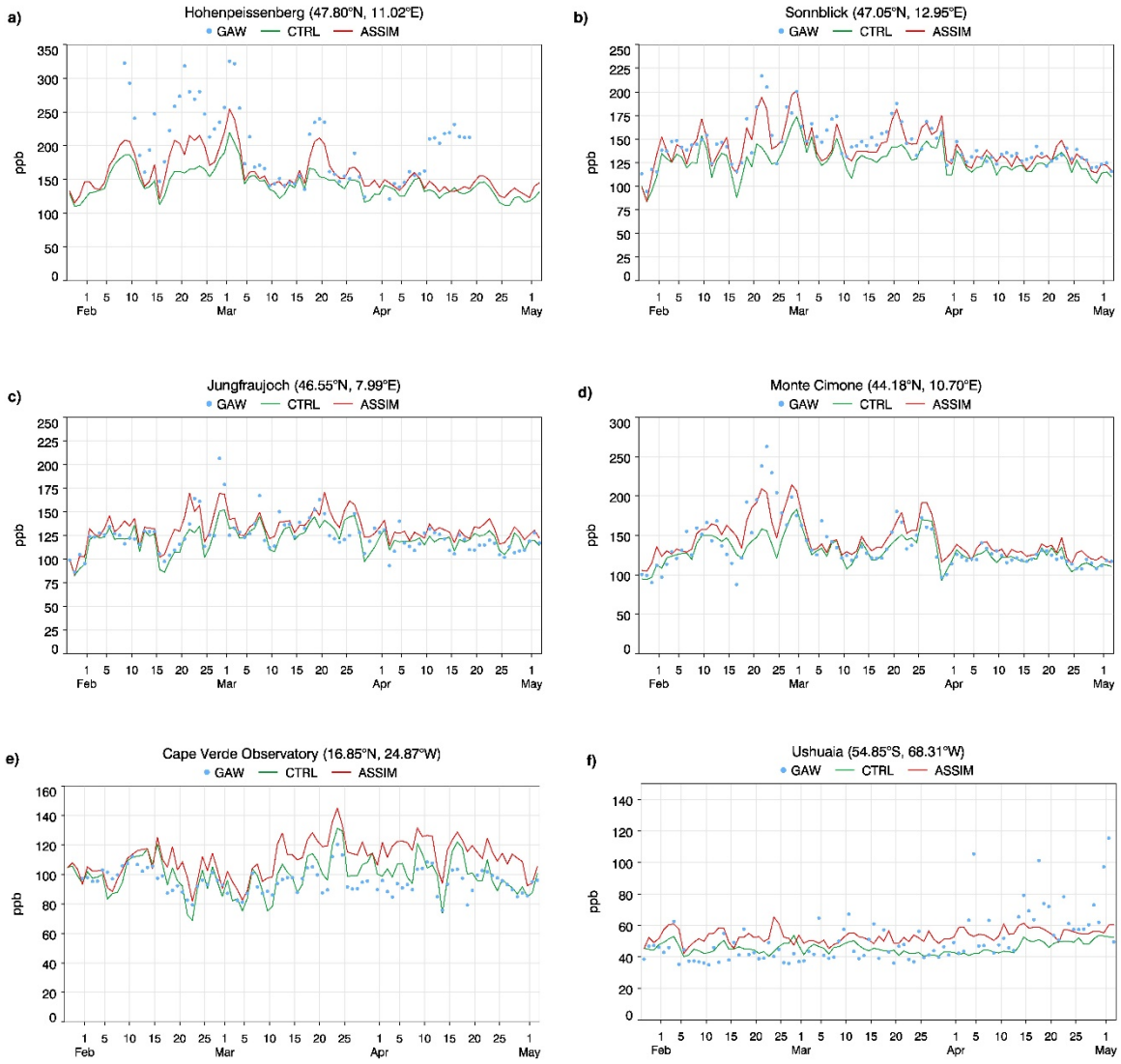

Figure 16: Timeseries of daily surface CO from GAW (blue dots), ASSIM (red) and CTRL (green) in ppb at (a) Hohenpeissenberg, (b) Sonnblick, (c) Jungfraujoch, (d) Monte Cimone, (e) Cape Verde Observatory and Ushuaia.